Chapter 19
Crystal Plasticity

The crystal plasticity analysis requires the calculation of the slips in numerous slip systems. Therefore, it could not be realized by the concept of the conventional elastoplasticity with the yield surface enclosing a purely-elastic domain, since it requires the yield judgment and the operation to pull-back the resolved shear stress to the critical shear stress. Then, unfortunately the creep crystal-plasticity model proposed by Peirce et al. (1982, 1983) is used widely. It is impertinent such that the creep shear strain rate is always induced even for the state that the resolved shear stress is unloaded from the critical shear stress as known from the defect of the creep model described in Sect. 13.3.

The crystal plasticity analysis can be attained appropriately by introducing the concept of the subloading surface which is endowed with the distinguished advantages: (1) Yield judgment is not required and (2) Automatic controlling function to attract the stress to the yield surface in the plastic loading process is furnished as described in Chaps. 7, 8, and 9. The pertinent formulation for the crystal plasticity analysis based on the subloading concept will be given in this chapter.

19.1 Multiplicative Decomposition of Deformation Gradient Tensor

The intermediate configuration is obtained by excluding the rigid-body rotation in addition to the elastic deformation from the current configuration as was postulated in Chaps. 6 and 12. Therefore, the intermediate configuration is independent of the rigid-body rotation. Consequently, the deformation gradient $\mathbf{F}$ is multiplicatively decomposed into the elastic deformation gradient $\mathbf{F}^e$ composed of the substructure rotation tensor $\mathbf{R}^e$ involving the rigid-body rotation and the right elastic stretch tensor $\mathbf{U}^e$ and the plastic deformation gradient $\mathbf{F}^p$ as follows (see Fig. 19.1):

K. Hashiguchi, *Foundations of Elastoplasticity: Subloading Surface Model*,
DOI 10.1007/978-3-319-48821-9_19

$$d\mathbf{x} = \mathbf{R}^e d\tilde{\mathbf{x}} = \mathbf{R}^e \mathbf{U}^e d\overline{\mathbf{X}} = \mathbf{F}^e d\overline{\mathbf{X}} = \mathbf{F} d\mathbf{X} \tag{19.1}$$

$$\left.\begin{array}{l} d\tilde{\mathbf{x}} = \mathbf{U}^e d\overline{\mathbf{X}} = \mathbf{U}^e \mathbf{F}^p d\mathbf{X} \\ d\overline{\mathbf{X}} = \mathbf{F}^p d\mathbf{X} \end{array}\right\} \tag{19.2}$$

Then, it follows that

$$\boxed{\mathbf{F} = \mathbf{F}^e \mathbf{F}^p = \mathbf{R}^e \mathbf{U}^e \mathbf{F}^p} \tag{19.3}$$

$$\mathbf{F}^e = \mathbf{R}^e \mathbf{U}^e = \mathbf{V}^e \mathbf{R}^e \tag{19.4}$$

$$\mathbf{F}^p = \mathbf{R}^p \mathbf{U}^p = \mathbf{V}^p \mathbf{R}^p \tag{19.5}$$

where $\mathbf{X}$, $\mathbf{x}$ and $\overline{\mathbf{X}}$ are the position vectors of material particles in the initial (reference), the current and the intermediate configuration, respectively. $\tilde{\mathbf{x}}$ is the position vector of material particle in the configuration pulled-back by the substructure rotation $\mathbf{R}^e$ from the current configuration.

The initial and the current configurations are designated by $\mathcal{K}_0$ and $\mathcal{K}$, respectively, and the configurations pulled-back from the current configuration by the substructure rotation $\mathbf{R}^e$ and by the elastic deformation gradient $\mathbf{F}^e$ are designated as $\widetilde{\mathcal{K}}$ and $\overline{\mathcal{K}}$, respectively, as shown in Fig. 19.1.

19.2 Strain Rate and Spin

The following decomposition is obtained from Eq. (19.2).

$$\boldsymbol{l} = \boldsymbol{l}^e + \boldsymbol{l}^p \tag{19.6}$$

where

$$\left.\begin{array}{l} \boldsymbol{l} \equiv \dfrac{\partial \boldsymbol{v}}{\partial \mathbf{x}} = \dot{\mathbf{F}}\mathbf{F}^{-1}, \\ \boldsymbol{l}^e \equiv \dot{\mathbf{F}}^e \mathbf{F}^{e-1}, \boldsymbol{l}^p \equiv \mathbf{F}^e \overline{\mathbf{L}}^p \mathbf{F}^{e-1} \\ \overline{\mathbf{L}}^p \equiv \dot{\mathbf{F}}^p \mathbf{F}^{p-1} \end{array}\right\} \tag{19.7}$$

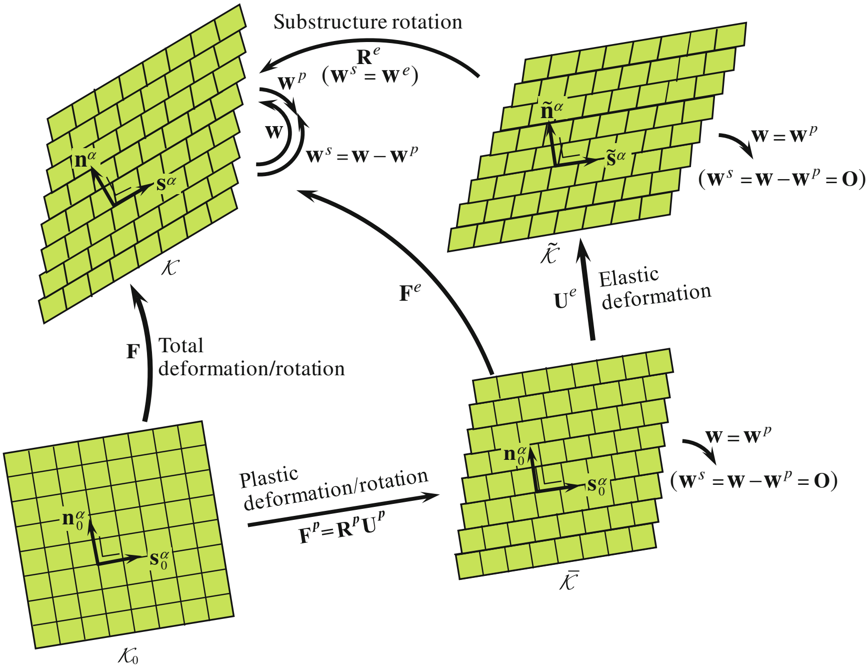

Fig. 19.1 Multiplicative decomposition in crystal plasticity based on isoclinic concept (Mandel 1973, 1974)

Further, the following additive decompositions to the symmetric and the anti-symmetric parts hold.

$$\left.\begin{aligned} \boldsymbol{l} &= \mathbf{d} + \mathbf{w} \\ \boldsymbol{l}^e &= \mathbf{d}^e + \mathbf{w}^e \\ \boldsymbol{l}^p &= \mathbf{d}^p + \mathbf{w}^p \\ \overline{\mathbf{L}}^p &= \overline{\mathbf{D}}^p + \overline{\mathbf{W}}^p \end{aligned}\right\} \tag{19.8}$$

with

$$\left.\begin{aligned} \mathbf{d} &= \mathbf{d}^e + \mathbf{d}^p \\ \mathbf{w} &= \mathbf{w}^e + \mathbf{w}^p \end{aligned}\right\} \tag{19.9}$$

where

$$\left.\begin{array}{ll}\mathbf{d}=\mathrm{sym}[\boldsymbol{l}]=\mathrm{sym}[\dot{\mathbf{F}}\mathbf{F}^{-1}], & \mathbf{w}=\mathrm{ant}[\boldsymbol{l}]=\mathrm{ant}[\dot{\mathbf{F}}\mathbf{F}^{-1}]\\ \mathbf{d}^e=\mathrm{sym}[\boldsymbol{l}^e]=\mathrm{sym}[\dot{\mathbf{F}}^e\mathbf{F}^{e-1}], & \mathbf{w}^e=\mathrm{ant}[\boldsymbol{l}^e]=\mathrm{ant}[\dot{\mathbf{F}}^e\mathbf{F}^{e-1}]\\ \overline{\mathbf{D}}^p=\mathrm{sym}\left[\overline{\mathbf{L}}^p\right]=\mathrm{sym}[\dot{\mathbf{F}}^p\mathbf{F}^{p-1}], & \overline{\mathbf{W}}^p=\mathrm{ant}\left[\overline{\mathbf{L}}^p\right]=\mathrm{ant}[\dot{\mathbf{F}}^p\mathbf{F}^{p-1}]\\ \mathbf{d}^p=\mathrm{sym}[\boldsymbol{l}^p]=\mathrm{sym}[\mathbf{F}^e\overline{\mathbf{L}}^p\mathbf{F}^{e-1}], & \mathbf{w}^p=\mathrm{ant}[\boldsymbol{l}^p]=\mathrm{ant}[\mathbf{F}^e\overline{\mathbf{L}}^p\mathbf{F}^{e-1}]\end{array}\right\} \tag{19.10}$$

Now, adopt the embedded base $(\mathbf{g}_1, \mathbf{g}^2, \mathbf{g}_3)$ described in Sect. 4.4. Here, the first primary base vector $\mathbf{g}_1$ is chosen parallel to the crystal lattice and denoted by $\mathbf{s}^\alpha$ and the secondary reciprocal base vector $\mathbf{g}^2$ by $\mathbf{n}^\alpha$ in the slip system α, satisfying $\mathbf{s}^\alpha \bullet \mathbf{n}^\alpha = 0$ by Eq. $(4.30)_2$ while they are called the *lattice vectors*, *director frame, director triad*, *isoclinic triad*, etc. Limiting to the two-dimensional deformation, $\mathbf{g}_3 (= \mathbf{g}^3)$ is the unit vector $(||\mathbf{g}_3|| = 1)$ and chosen perpendicular to the base vectors $\mathbf{s}^\alpha$ and $\mathbf{n}^\alpha$. Further, the base vectors $\mathbf{s}^\alpha$ and $\mathbf{n}^\alpha$ in the initial configuration are chosen to be the unit vectors and denoted by the symbols $\mathbf{s}_0^\alpha$ and $\mathbf{n}_0^\alpha$ $(||\mathbf{s}_0^\alpha|| = ||\mathbf{n}_0^\alpha|| = 1)$, respectively, which correspond to the reference base vectors $\mathbf{G}_1$ and $\mathbf{G}^2$, respectively, in Sect. 4.4. Reminding the aforementioned assumption that the intermediate configuration is independent of the rigid-body rotation and noting the simple shear deformation along the crystalline lattice under the plastic incompressibility, the base vectors are kept unchanged as $\mathbf{s}_0^\alpha$ and $\mathbf{n}_0^\alpha$ in the process from the initial to the intermediate configurations (see Fig. 19.1). This physical consequence is referred to as the *isoclinic concept* by Mandel (1973, 1974), while "isoclinic" is the Greek word meaning "same (or constant) direction" as was described in Sect. 6.1.

The current primary base vector $\mathbf{s}^\alpha$ and its reciprocal base vector $\mathbf{n}^\alpha$ are related to the initial base vectors $\mathbf{s}_0^\alpha$ and $\mathbf{n}_0^\alpha$ by Eqs. (4.32) and (4.35), replacing $\mathbf{F}$ to $\mathbf{F}^e$, as follows:

$$\left.\begin{array}{l}\mathbf{s}^\alpha=\mathbf{F}^e\mathbf{s}_0^\alpha=\mathbf{s}_0^\alpha\mathbf{F}^{eT},\ \mathbf{s}_0^\alpha=\mathbf{F}^{e-1}\mathbf{s}^\alpha=\mathbf{s}^\alpha\mathbf{F}^{e-T}\\ \mathbf{n}^\alpha=\mathbf{F}^{e-T}\mathbf{n}_0^\alpha=\mathbf{n}_0^\alpha\mathbf{F}^{e-1},\ \mathbf{n}_0^\alpha=\mathbf{F}^{eT}\mathbf{n}^\alpha=\mathbf{n}^\alpha\mathbf{F}^e\\ (\mathbf{s}^\alpha\bullet\mathbf{n}^\alpha=\mathbf{F}^e\mathbf{s}_0^\alpha\bullet\mathbf{F}^{e-T}\mathbf{n}_0^\alpha=\mathbf{s}_0^\alpha\bullet\mathbf{F}^{eT}\mathbf{F}^{e-T}\mathbf{n}_0^\alpha=\mathbf{s}_0^\alpha\bullet\mathbf{n}_0^\alpha=0)\end{array}\right\} \tag{19.11}$$

noting $\mathbf{T}\mathbf{v} = \mathbf{v}\mathbf{T}^T (T_{ij}v_j = v_jT_{ij})$. The base vectors $\tilde{\mathbf{s}}^\alpha$ and $\tilde{\mathbf{n}}^\alpha$ obtained by excluding the substructure rotation from the current configuration as shown in Fig. 19.1 are related to the initial base vectors $\mathbf{s}_0^\alpha$ and $\mathbf{n}_0^\alpha$ by replacing $\mathbf{F}^e$ to $\mathbf{R}^e$ in Eq. (19.11).

The rates of $\mathbf{s}^\alpha$ and $\mathbf{n}^\alpha$ are given as follows:

$$\left.\begin{array}{l}\dot{\mathbf{s}}^\alpha=\dot{\mathbf{F}}^e\mathbf{s}_0^\alpha=\dot{\mathbf{F}}^e\mathbf{F}^{e-1}\mathbf{s}^\alpha=\boldsymbol{l}^e\mathbf{s}^\alpha=\mathbf{s}^\alpha\boldsymbol{l}^{eT}\\ \dot{\mathbf{n}}^\alpha=\dot{\mathbf{F}}^{e-T}\mathbf{n}_0^\alpha=\dot{\mathbf{F}}^{e-T}\mathbf{F}^{eT}\mathbf{n}^\alpha=-\boldsymbol{l}^{eT}\mathbf{n}^\alpha=-\mathbf{n}^\alpha\boldsymbol{l}^e\end{array}\right\} \tag{19.12}$$

Needless to say, the current base vectors $(\mathbf{s}^\alpha, \mathbf{n}^\alpha)$ and $(\tilde{\mathbf{s}}^\alpha, \tilde{\mathbf{n}}^\alpha)$ are no longer unit vectors.

On the other hand, the simple shear strain γ^α along the slip system α is additively decomposed into the elastic shear strain $\gamma^{e\alpha}$ and the plastic shear strain $\gamma^{p\alpha}$ as follows:

$$\gamma^{\alpha} = \gamma^{e\alpha} + \gamma^{p\alpha}, \quad \overset{\bullet}{\gamma}^{\alpha} = \overset{\bullet}{\gamma}^{e\alpha} + \overset{\bullet}{\gamma}^{p\alpha} \tag{19.13}$$

The difference of plastic displacements, $d\mathbf{u}^{p\alpha}$, in both ends of infinitesimal line element $d\mathbf{X}$, which is induced by plastic shear strain γ^{α} in slip system α, is given by the following equation (see Fig. 19.2).

$$d\mathbf{u}^{p\alpha} = \gamma^{p\alpha}(\mathbf{n}_0^{\alpha} \cdot d\mathbf{X})\mathbf{s}_0^{\alpha} = \gamma^{p\alpha}\mathbf{s}_0^{\alpha} \otimes \mathbf{n}_0^{\alpha} d\mathbf{X} \tag{19.14}$$

Then, $d\mathbf{X}$ changes to

$$d\overline{\mathbf{X}} = d\mathbf{X} + d\mathbf{u}^{p\alpha} = (\mathbf{I} + \gamma^{p\alpha}\mathbf{s}_0^{\alpha} \otimes \mathbf{n}_0^{\alpha})d\mathbf{X} \tag{19.15}$$

in the intermediate configuration.

Noting Eqs. (19.1)$_3$ and (19.15), one has

$$\mathbf{F}^{p\alpha} = \mathbf{I} + \gamma^{p\alpha}\mathbf{s}_0^{\alpha} \otimes \mathbf{n}_0^{\alpha}, \quad \mathbf{F}^{p\alpha-1} = \mathbf{I} - \gamma^{p\alpha}\mathbf{s}_0^{\alpha} \otimes \mathbf{n}_0^{\alpha} \tag{19.16}$$

by virtue of $(\mathbf{I} + \gamma^{p\alpha}\mathbf{s}_0^{\alpha} \otimes \mathbf{n}_0^{\alpha})(\mathbf{I} - \gamma^{p\alpha}\mathbf{s}_0^{\alpha} \otimes \mathbf{n}_0^{\alpha}) = \mathbf{I}$ due to $\mathbf{n}_0^{\alpha} \cdot \mathbf{s}_0^{\alpha} = 0$. Further, noting

$$(\mathbf{I} + \gamma^{p\alpha}\mathbf{s}_0^{\alpha} \otimes \mathbf{n}_0^{\alpha})^{\bullet}(\mathbf{I} - \gamma^{p\alpha}\mathbf{s}_0^{\alpha} \otimes \mathbf{n}_0^{\alpha}) = \overset{\bullet}{\gamma}^{p\alpha}\mathbf{s}_0^{\alpha} \otimes \mathbf{n}_0^{\alpha} - \overset{\bullet}{\gamma}^{p\alpha}\mathbf{s}_0^{\alpha} \otimes \mathbf{n}_0^{\alpha}\gamma^{p\alpha}\mathbf{s}_0^{\alpha} \otimes \mathbf{n}_0^{\alpha} \tag{19.17}$$

it follows that

$$\dot{\mathbf{F}}^{p\alpha}\mathbf{F}^{p\alpha-1} = \overset{\bullet}{\gamma}^{p\alpha}\mathbf{s}_0^{\alpha} \otimes \mathbf{n}_0^{\alpha} \tag{19.18}$$

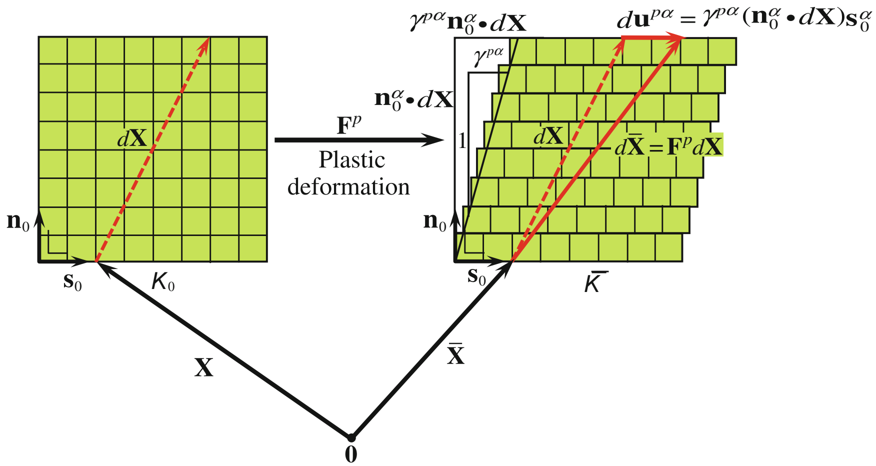

Fig. 19.2 Plastic displacement in end of infinitesimal line element $d\mathbf{X}$, which is induced by plastic shear strain in slip system

The plastic velocity gradient based in the intermediate configuration is given by summing the plastic velocity gradients induced in all the relevant slip systems as follows:

$$\overline{\mathbf{L}}^{p} = \sum_{\beta=1}^{n} \dot{\mathbf{F}}^{p\beta}\mathbf{F}^{p\beta-1} = \sum_{\beta=1}^{n} \mathbf{s}_0^{\beta} \otimes \mathbf{n}_0^{\beta}\dot{\gamma}^{p\beta} \tag{19.19}$$

where n is the number of slip systems. The substitution of Eq. (19.19) into Eq. (19.10) leads to

$$\left.\begin{aligned} \overline{\mathbf{D}}^{p} &= \sum_{\beta=1}^{n} \overline{\mathbf{P}}^{\beta}\dot{\gamma}^{p\beta} \\ \overline{\mathbf{W}}^{p} &= \sum_{\beta=1}^{n} \overline{\mathbf{Q}}^{\beta}\dot{\gamma}^{p\beta} \end{aligned}\right\} \tag{19.20}$$

where

$$\left.\begin{aligned} \overline{\mathbf{P}}^{\alpha} &= \mathrm{sym}[\mathbf{s}_0^{\alpha} \otimes \mathbf{n}_0^{\alpha}] \\ \overline{\mathbf{Q}}^{\alpha} &= \mathrm{ant}[\mathbf{s}_0^{\alpha} \otimes \mathbf{n}_0^{\alpha}] \end{aligned}\right\} \tag{19.21}$$

Substituting Eq. (19.19) with Eq. (19.11) into Eq. (19.7) reads:

$$\boldsymbol{l}^{p} = \sum_{\beta=1}^{n} \mathbf{s}^{\beta} \otimes \mathbf{n}^{\beta}\dot{\gamma}^{p\beta} \tag{19.22}$$

Inserting Eq. (19.22) into Eq. (19.10), one has

$$\left.\begin{aligned} \mathbf{d}^{p} &= \sum_{\beta=1}^{n} \mathbf{p}^{\beta}\dot{\gamma}^{p\beta} \\ \mathbf{w}^{p} &= \sum_{\alpha=1}^{n} \mathbf{q}^{\beta}\dot{\gamma}^{p\beta} \end{aligned}\right\} \tag{19.23}$$

with

$$\left.\begin{aligned} \mathbf{p}^{\alpha} &= \mathrm{sym}[\mathbf{s}^{\alpha} \otimes \mathbf{n}^{\alpha}] \\ \mathbf{q}^{\alpha} &= \mathrm{ant}[\mathbf{s}^{\alpha} \otimes \mathbf{n}^{\alpha}] \end{aligned}\right\} \tag{19.24}$$

Substituting Eq. (19.22) into Eq. (19.6), one has

$$\boldsymbol{l}^e = \boldsymbol{l} - \boldsymbol{l}^p = \boldsymbol{l} - \sum_{\beta=1}^{n} \mathbf{s}^\beta \otimes \mathbf{n}^\beta \dot{\gamma}^{p\beta} = \boldsymbol{l} - \sum_{\beta=1}^{n} (\mathbf{p}^\beta + \mathbf{q}^\beta)\dot{\gamma}^{p\beta} \tag{19.25}$$

$$\left.\begin{aligned} \mathbf{d}^e &= \mathrm{sym}[\boldsymbol{l}^e] = \mathrm{sym}[\dot{\mathbf{F}}^e \mathbf{F}^{e-1}] = \mathbf{d} - \sum_{\beta=1}^{n} \mathbf{p}^\beta \dot{\gamma}^{p\beta} \\ \mathbf{w}^e &= \mathrm{ant}[\boldsymbol{l}^e] = \mathrm{ant}[\dot{\mathbf{F}}^e \mathbf{F}^{e-1}] = \mathbf{w} - \sum_{\beta=1}^{n} \mathbf{q}^\beta \dot{\gamma}^{p\beta} \end{aligned}\right\} \tag{19.26}$$

19.3 Resolved Shear Stress (Rate)

Let the resolved shear stress be defined as follows (Asaro and Rice 1977):

$$\tau^\alpha = \mathbf{s}^\alpha \cdot \boldsymbol{\tau} \mathbf{n}^\alpha = \mathbf{p}^\alpha : \boldsymbol{\tau} \tag{19.27}$$

The time-differentiation of Eq. (19.27) leads to

$$\dot{\tau}^\alpha = \dot{\mathbf{s}}^\alpha \cdot \boldsymbol{\tau} \boldsymbol{n}^\alpha + \mathbf{s}^\alpha \cdot \dot{\boldsymbol{\tau}} \mathbf{n}^\alpha + \mathbf{s}^\alpha \cdot \boldsymbol{\tau} \dot{\mathbf{n}}^\alpha$$

Substituting Eqs. (19.8) and (19.12), the right-hand side of this equation leads:

$$\begin{aligned} &\dot{\mathbf{s}}^\alpha \cdot \boldsymbol{\tau} \mathbf{n}^\alpha + \mathbf{s}^\alpha \cdot \dot{\boldsymbol{\tau}} \mathbf{n}^\alpha + \mathbf{s}^\alpha \cdot \boldsymbol{\tau} \dot{\mathbf{n}}^\alpha \\ &\quad = (\mathbf{d}^e + \mathbf{w}^e)\mathbf{s}^\alpha \cdot \boldsymbol{\tau} \mathbf{n}^\alpha + \mathbf{s}^\alpha \cdot \dot{\boldsymbol{\tau}} \mathbf{n}^\alpha - \mathbf{s}^\alpha \cdot \boldsymbol{\tau} (\mathbf{d}^e + \mathbf{w}^e)^T \mathbf{n}^\alpha \\ &\quad = \mathbf{s}^\alpha \cdot (\mathbf{d}^e + \mathbf{w}^e)^T \boldsymbol{\tau} \mathbf{n}^\alpha + \mathbf{s}^\alpha \cdot \dot{\boldsymbol{\tau}} \mathbf{n}^\alpha - \mathbf{s}^\alpha \cdot \boldsymbol{\tau} (\mathbf{d}^e - \mathbf{w}^e) \mathbf{n}^\alpha \\ &\quad = \mathbf{s}^\alpha \cdot (\dot{\boldsymbol{\tau}} - \mathbf{w}^e \boldsymbol{\tau} + \boldsymbol{\tau} \mathbf{w}^e + \mathbf{d}^e \boldsymbol{\tau} - \boldsymbol{\tau} \mathbf{d}^e) \mathbf{n}^\alpha \end{aligned}$$

leading to

$$\dot{\tau}^\alpha = \mathbf{s}^\alpha \cdot \overset{*}{\boldsymbol{\tau}} \mathbf{n}^\alpha + \mathbf{s}^\alpha \cdot (\mathbf{d}^e \boldsymbol{\tau} - \boldsymbol{\tau} \mathbf{d}^e) \mathbf{n}^\alpha \tag{19.28}$$

where (*) designates the corotational rate based on the spin of crystal lattice subjected to the rigid-body rotation and elastic rotation and $\overset{*}{\boldsymbol{\tau}}$ is given by

$$\overset{*}{\boldsymbol{\tau}} = \mathbf{R}^e (\mathbf{R}^{eT} \boldsymbol{\tau} \mathbf{R}^e)^{\bullet} \mathbf{R}^{eT} = \dot{\boldsymbol{\tau}} - \mathbf{w}^e \boldsymbol{\tau} + \boldsymbol{\tau} \mathbf{w}^e = \mathbf{E} : \mathbf{d}^e \tag{19.29}$$

E being the overall elastic modulus tensor.

Taking account of Eqs. (19.24) and (19.52) and the symmetry of $\boldsymbol{\tau}$ and $\mathbf{d}^e$, one has

$$\begin{aligned}\mathbf{s}^{\alpha}\bullet\overset{*}{\boldsymbol{\tau}}\mathbf{n}^{\alpha} &= s_i^{\alpha}\overset{*}{\tau}_{ij}n_j^{\alpha} = s_i^{\alpha}n_j^{\alpha}\overset{*}{\tau}_{ij} = \mathbf{s}^{\alpha}\otimes\mathbf{n}^{\alpha}:\overset{*}{\boldsymbol{\tau}} = \mathbf{p}^{\alpha}:\overset{*}{\boldsymbol{\tau}}\\ &= \mathbf{p}^{\alpha}:\mathbf{E}:\mathbf{d}^{e} = p_{ij}^{\alpha}E_{ijkl}d_{kl}^{e} = E_{klij}p_{ij}^{\alpha}d_{kl}^{e} = \mathbf{E}\mathbf{p}^{\alpha}:\mathbf{d}^{e}\end{aligned}$$

$$\begin{aligned}\mathbf{s}^{\alpha}\bullet(\mathbf{d}^{e}\boldsymbol{\tau}-\boldsymbol{\tau}\mathbf{d}^{e})\mathbf{n}^{\alpha} &= s_i^{\alpha}d_{ir}^{e}\tau_{rs}n_s^{\alpha} - s_i^{\alpha}\tau_{ir}d_{rs}^{e}n_s^{\alpha}\\ &= \frac{1}{2}[(s_i^{\alpha}n_s^{\alpha}\tau_{sr})d_{ir}^{e} + (\tau_{rs}n_s^{\alpha}s_i^{\alpha})d_{ri}^{e}] - \frac{1}{2}[(n_s^{\alpha}s_i^{\alpha}\tau_{ir})d_{sr}^{e} + (\tau_{ri}s_i^{\alpha}n_s^{\alpha})d_{rs}^{e}]\\ &= \frac{1}{2}\{[(\mathbf{s}^{\alpha}\otimes\mathbf{n}^{\alpha})\boldsymbol{\tau}]:\mathbf{d}^{e} - [(\mathbf{n}^{\alpha}\otimes\mathbf{s}^{\alpha})\boldsymbol{\tau}]:\mathbf{d}^{e}\} - \frac{1}{2}\{[\boldsymbol{\tau}(\mathbf{s}^{\alpha}\otimes\mathbf{n}^{\alpha})]:\mathbf{d}^{e}\\ &\quad - [\boldsymbol{\tau}(\mathbf{n}^{\alpha}\otimes\mathbf{s}^{\alpha})]:\mathbf{d}^{e}\}\\ &= \left[\frac{1}{2}(\mathbf{s}^{\alpha}\otimes\mathbf{n}^{\alpha} - \mathbf{n}^{\alpha}\otimes\mathbf{s}^{\alpha})\boldsymbol{\tau} - \boldsymbol{\tau}\frac{1}{2}(\mathbf{s}^{\alpha}\otimes\mathbf{n}^{\alpha} - \mathbf{n}^{\alpha}\otimes\mathbf{s}^{\alpha}\right]:\mathbf{d}^{e}\\ &= (\mathbf{q}^{\alpha}\boldsymbol{\tau} - \boldsymbol{\tau}\mathbf{q}^{\alpha}):\mathbf{d}^{e} = \boldsymbol{\beta}^{\alpha}:\mathbf{d}^{e}\end{aligned}$$

Substituting these relations into Eq. (19.28), we have the relation between the resolved shear stress rate versus the global elastic strain rate as follows:

$$\overset{\bullet}{\tau}^{\alpha} = \boldsymbol{\Xi}^{\alpha}:\mathbf{d}^{e} \tag{19.30}$$

where

$$\boldsymbol{\Xi}^{\alpha} \equiv \mathbf{E}:\mathbf{p}^{\alpha} + \boldsymbol{\beta}^{\alpha}(\neq \boldsymbol{\Xi}^{\alpha T}) \tag{19.31}$$

Further, substituting Eq. $(19.26)_1$ into Eq. (19.30) reads:

$$\overset{\bullet}{\tau}^{\alpha} = \boldsymbol{\Xi}^{\alpha}:(\mathbf{d} - \sum_{\beta=1}^{n}\mathbf{p}^{\beta}\overset{\bullet}{\gamma}^{p\beta}) \tag{19.32}$$

19.4 Plastic Shear Strain Rate

The crystal shear yield condition describing the *crystal shear yield region* in the slip system α is given by

$$|\hat{\tau}^{\alpha}| = \tau_y^{\alpha} \tag{19.33}$$

where

$$\hat{\tau}^{\alpha} \equiv \tau^{\alpha} - \chi^{\alpha} \tag{19.34}$$

χ^{α} is the shear kinematic hardening variable and $\tau_y^{\alpha}\,(>0)$ is the shear hardening function, referred to as the *critical shear stress*, in the slip system α.

The associated flow rule to the subloading shear region is adopted for the plastic shear strain rate as follows:

$$\overset{\bullet}{\gamma}^{p\alpha} = \overset{\bullet}{\lambda}^{\alpha}\hat{n}^{\alpha} \ (\overset{\bullet}{\lambda}^{\alpha} \geq 0)(|\overset{\bullet}{\gamma}^{p\alpha}| = \overset{\bullet}{\lambda}^{\alpha}) \tag{19.35}$$

where

$$\hat{n}^{\alpha} \equiv \frac{\partial|\hat{\tau}^{\alpha}|}{\partial\tau^{\alpha}} = \frac{\hat{\tau}^{\alpha}}{|\hat{\tau}^{\alpha}|} = \mathrm{sign}(\hat{\tau}^{\alpha}) \ (|\hat{n}^{\alpha}| = 1) \tag{19.36}$$

The material-time derivative of Eq. (19.33) reads:

$$\hat{n}^{\alpha}(\overset{\bullet}{\tau}^{\alpha} - \overset{\bullet}{\chi}^{\alpha}) = \overset{\bullet}{\tau}_{y}^{\alpha} \tag{19.37}$$

i.e.

$$\overset{\bullet}{\tau}^{\alpha} = \hat{n}^{\alpha}\overset{\bullet}{\tau}_{y}{}^{\alpha} + \overset{\bullet}{\chi}^{\alpha} \tag{19.38}$$

The rate of critical shear stress is specified by

$$\overset{\bullet}{\tau}_{y}{}^{\alpha} = \sum_{\beta=1}^{n} h_{\alpha\beta}|\overset{\bullet}{\gamma}^{p\beta}| = \sum_{\beta=1}^{n} h_{\alpha\beta}\overset{\bullet}{\lambda}^{\beta} \tag{19.39}$$

where $h_{\alpha\beta}$ is given by the following matrix which is the function of the plastic shear strain (Peirce et al. 1982).

$$h_{\alpha\beta} = qh(\gamma^{p}) + (1-q)h(\gamma^{p})\delta_{\alpha\beta}(= h_{\beta\alpha}) = \begin{cases} h(\gamma^{p}) & \text{for} \quad \alpha = \beta \\ qh(\gamma^{p}) & \text{for} \quad \alpha \neq \beta \end{cases} (1 \leq q \leq 1.4) \tag{19.40}$$

$h(\gamma^{p})$ is given by the functional form

$$h(\gamma^{p}) = h_0 \mathrm{sech}^2\left(\frac{h_0\gamma^{p}}{\tau_s - \tau_{y0}}\right) \tag{19.41}$$

with

$$\gamma^{p} \equiv \sum_{\beta=1}^{n} \int_0^t |\overset{\bullet}{\gamma}^{p\beta}| dt \tag{19.42}$$

h_0 and τ_{y0} are the initial values of h and τ_y^{α}, i.e. $h_0 = h(0)$ and $\tau_{y0} = \tau_y^{\alpha}(0)$, respectively, and τ_s is the saturation value of τ_y^{α}, i.e. $\tau_s = \tau_y^{\alpha}(\infty)$.

Assume the following shear nonlinear-kinematic hardening rule.

$$\overset{\bullet}{\chi}{}^{\alpha} = c_\chi\left(\overset{\bullet}{\gamma}{}^{p\alpha} - \frac{1}{\zeta_\chi \tau_y^\alpha}|\overset{\bullet}{\gamma}{}^{p\alpha}|\chi^\alpha\right) = c_\chi \overset{\bullet}{\lambda}{}^{\alpha}\left(\hat{n}^\alpha - \frac{1}{\zeta_\chi \tau_y^\alpha}\chi^\alpha\right) \tag{19.43}$$

where c_χ and ζ_χ are the material constants. The latent hardening may be incorporated for the shear kinematic hardening (e.g. Bassani and Wu 1991; Harder 1999; Xu and Jiang 2004).

Substituting Eqs. (19.39) and (19.43) into Eq. (19.38), one has the consistency condition for the subloading crystalline shear region.

$$\overset{\bullet}{\tau}{}^{\alpha} = \hat{n}^\alpha \sum_{\beta=1}^{n} h_{\alpha\beta}\overset{\bullet}{\lambda}{}^{\beta} + c_\chi\left(\hat{n}^\alpha - \frac{1}{\zeta_\chi \tau_y^\alpha}\chi^\alpha\right)\overset{\bullet}{\lambda}{}^{\alpha} \tag{19.44}$$

which is rewritten as

$$\overset{\bullet}{\tau}{}^{\alpha} = \sum_{\beta=1}^{n} \bar{h}_{\alpha\beta}\overset{\bullet}{\lambda}{}^{\beta} \tag{19.45}$$

where

$$\bar{h}_{\alpha\beta} \equiv \hat{n}^\alpha h_{\alpha\beta} + c_\chi\left(\hat{n}^\alpha - \frac{1}{\zeta_\chi \tau_y^\alpha}\chi^\alpha\right)\delta_{\alpha\beta}(\neq \bar{h}_{\beta\alpha}) \tag{19.46}$$

19.5 Strain Rate Versus Stress Rate Relations

The global constitutive relation is given by Eq. (19.29) i.e.

$$\overset{*}{\boldsymbol{\tau}} = \mathbf{E} : \mathbf{d}^e \tag{19.47}$$

On the other hand, the Jaumann rate of the Kirchhoff stress is given as

$$\overset{\circ}{\boldsymbol{\tau}}{}^{w} = \overset{\bullet}{\boldsymbol{\tau}} - \mathbf{w}\boldsymbol{\tau} + \boldsymbol{\tau}\mathbf{w} \tag{19.48}$$

These corotational rates are related as

$$\overset{*}{\boldsymbol{\tau}} = \overset{\circ}{\boldsymbol{\tau}}{}^{w} + \mathbf{w}^p\boldsymbol{\tau} - \boldsymbol{\tau}\mathbf{w}^p \tag{19.49}$$

noting

$$\dot{\boldsymbol{\tau}} - \mathbf{w}^e \boldsymbol{\tau} + \boldsymbol{\tau} \mathbf{w}^e = \dot{\boldsymbol{\tau}} - (\mathbf{w} - \mathbf{w}^p) \boldsymbol{\tau} + \boldsymbol{\tau} (\mathbf{w} - \mathbf{w}^p). \tag{19.50}$$

The substitution of Eq. (19.23) into Eq. (19.49) leads to

$$\overset{*}{\boldsymbol{\tau}} = \overset{\circ}{\boldsymbol{\tau}}{}^w + \sum_{\beta=1}^{n} \boldsymbol{\beta}^\beta \dot{\gamma}^{p\beta} \tag{19.51}$$

where

$$\boldsymbol{\beta}^\alpha \equiv \mathbf{q}^\alpha \boldsymbol{\tau} - \boldsymbol{\tau} \mathbf{q}^\alpha \; (= -\boldsymbol{\beta}^{\alpha T}) \tag{19.52}$$

Further, substituting Eqs. $(19.9)_1$ and $(19.23)_1$ into Eq. (19.47), one has

$$\overset{*}{\boldsymbol{\tau}} = \mathbf{E} : (\mathbf{d} - \mathbf{d}^p) = \mathbf{E} : \mathbf{d} - \sum_{\beta=1}^{n} \mathbf{E} : \mathbf{p}^\beta \dot{\gamma}^{p\beta} \tag{19.53}$$

The substitution of Eq. (19.53) into Eq. (19.51) reads:

$$\overset{\circ}{\boldsymbol{\tau}}{}^w = \mathbf{E} : \mathbf{d} - \sum_{\beta=1}^{n} \boldsymbol{\Xi}^\beta \dot{\gamma}^{p\beta} \tag{19.54}$$

The strain rate is described by the stress rates from Eq. (19.53) and with Eq. (19.51) as follows:

$$\mathbf{d} = \mathbf{E}^{-1} : \overset{*}{\boldsymbol{\tau}} + \sum_{\beta=1}^{n} \mathbf{p}^\beta \dot{\gamma}^{p\beta} = \mathbf{E}^{-1} : (\overset{\circ}{\boldsymbol{\tau}}{}^w + \sum_{\beta=1}^{n} \boldsymbol{\Xi}^\beta \dot{\gamma}^{p\beta}) \tag{19.55}$$

Equating Eq. (19.32) with Eq. (19.45), it follows that

$$\boldsymbol{\Xi}^\alpha : \left(\mathbf{d} - \sum_{\beta=1}^{n} \mathbf{p}^\beta \hat{n}^\beta \dot{\lambda}^\beta \right) = \sum_{\beta=1}^{n} \bar{h}_{\alpha\beta} \dot{\lambda}^\beta \tag{19.56}$$

which is rewritten as

$$\boldsymbol{\Xi}^\alpha : \mathbf{d} = \sum_{\beta=1}^{n} \overline{M}_{\alpha\beta} \dot{\lambda}^\beta \tag{19.57}$$

where

$$\overline{M}_{\alpha\beta} \equiv \bar{h}_{\alpha\beta} + \boldsymbol{\Xi}^{\alpha} : \mathbf{p}^{\beta}\hat{n}^{\beta} \ (\neq \overline{M}_{\alpha\beta}^{T}) \tag{19.58}$$

The plastic shear strain rate is given from Eq. (19.57) as follows:

$$\overset{\bullet}{\lambda}{}^{\alpha} = \sum_{\beta=1}^{n} \overline{M}_{\alpha\beta}^{-1} \boldsymbol{\Xi}^{\beta} : \mathbf{d} \ \left(\sum_{\beta=1}^{n} \overline{M}_{\alpha\beta} \overset{\bullet}{\lambda}{}^{\beta} = \boldsymbol{\Xi}^{\alpha} : \mathbf{d} \right) \tag{19.59}$$

Substituting Eq. (19.59) into Eq. (19.54), it follows that

$$\overset{\circ}{\boldsymbol{\tau}}{}^{w} = \mathbf{E} : \mathbf{d} - \sum_{\alpha=1}^{n} \boldsymbol{\Xi}^{\alpha} \overset{\bullet}{\lambda}{}^{\alpha} \hat{n}^{\alpha} = \mathbf{E} : \mathbf{d} - \sum_{\alpha=1}^{n} \boldsymbol{\Xi}^{\alpha} \hat{n}^{\alpha} \sum_{\beta=1}^{n} \overline{M}_{\alpha\beta}^{-1} \boldsymbol{\Xi}^{\beta} : \mathbf{d}$$

leading to

$$\overset{\circ}{\boldsymbol{\tau}}{}^{w} = \overline{\mathbf{K}}^{ep} : \mathbf{d} \tag{19.60}$$

where

$$\overline{\mathbf{K}}^{ep} \equiv \mathbf{E} - \sum_{\alpha=1}^{n} \sum_{\beta=1}^{n} \boldsymbol{\Xi}^{\alpha} \otimes \hat{n}^{\alpha} \overline{M}_{\alpha\beta}^{-1} \boldsymbol{\Xi}^{\beta} \ (\neq \bar{\mathbf{K}}^{epT}) \tag{19.61}$$

The loading criterion for the plastic shear strain rate is given by the sign of the plastic multiplier in terms of the shear strain rate as follows:

$$\left. \begin{array}{ll} \overset{\bullet}{\gamma}{}^{p\alpha} \neq 0 & \text{for } |\hat{\tau}^{\alpha}| = \tau_{y}^{\alpha} \ \text{ and } \ \tau^{\alpha} \overset{\bullet}{\tau}{}^{\alpha} > 0 \\ \overset{\bullet}{\gamma}{}^{p\alpha} = 0 & \text{for others} \end{array} \right\} \tag{19.62}$$

19.6 Uniqueness of Slip Rate Mode

Hill and Rice (1972) proved that the sufficient condition for the uniqueness of the combination of slip rates is the positive-definite of the matrix in Eq. (19.58) in all the slip systems as follows:

Suppose to impose the two strain rates $\mathbf{d}$ and $\bar{\mathbf{d}}$, and designate the slip rates for these strain rates as $\overset{\bullet}{\gamma}{}^{\alpha}$ and $\overset{\bullet}{\bar{\gamma}}{}^{\alpha}$, respectively, in the two slip modes, and denote their differences as follows:

$$\Delta\overset{\bullet}{\gamma}^{\alpha} = \overset{\bullet}{\gamma}^{\alpha} - \overset{\bullet}{\bar{\gamma}}^{\alpha} \tag{19.63}$$

$$\Delta\mathbf{d} = \mathbf{d} - \bar{\mathbf{d}} \tag{19.64}$$

The following inequality must be satisfied from Eqs. (19.38) and (19.39), ignoring the kinematic hardening for simplicity.

$$n^{\alpha}\overset{\bullet}{\tau}^{\alpha} \leq \sum_{\beta=1}^{n} \left(h_{\alpha\beta}\overset{\bullet}{\gamma}^{\beta} n^{\alpha}\right) \tag{19.65}$$

where

$$n^{\alpha} \equiv \frac{\partial|\tau^{\alpha}|}{\partial\tau^{\alpha}} = \frac{\tau^{\alpha}}{|\tau^{\alpha}|} = \mathrm{sign}(\tau^{\alpha}) \ (|n^{\alpha}| = 1) \tag{19.66}$$

The substitution of Eq. (19.32) into Eq. (19.65) leads to

$$\boldsymbol{\Xi}^{\alpha} : \left(\mathbf{d} - \sum_{\beta=1}^{n} \mathbf{p}^{\beta}\overset{\bullet}{\gamma}^{\beta}\right) n^{\alpha} \leq \sum_{\beta=1}^{n} \left(h_{\alpha\beta}\overset{\bullet}{\gamma}^{\beta} n^{\alpha}\right) \tag{19.67}$$

resulting in

$$\left[\boldsymbol{\Xi}^{\alpha} : \left(\mathbf{d} - \sum_{\beta=1}^{n} \mathbf{p}^{\beta}\overset{\bullet}{\gamma}^{\beta}\right) - \sum_{\beta=1}^{n} h_{\alpha\beta}\overset{\bullet}{\gamma}^{\beta}\right] n^{\alpha} \leq 0$$

which is described as

$$\left(\boldsymbol{\Xi}^{\alpha} : \mathbf{d} - \sum_{\beta=1}^{n} M_{\alpha\beta}\overset{\bullet}{\gamma}^{\beta}\right) n^{\alpha} \leq 0 \tag{19.68}$$

where

$$M_{\alpha\beta} \equiv h_{\alpha\beta} + \boldsymbol{\Xi}^{\alpha} : \mathbf{p}^{\beta} n^{\beta} \tag{19.69}$$

First, we assume that the slip system α is active in both modes, i.e. $\overset{\bullet}{\gamma}^{\alpha} \neq 0$, $\overset{\bullet}{\bar{\gamma}}^{\alpha} \neq 0$, so that the following equations hold from Eq. (19.68).

$$\left.\begin{array}{l} \left(\boldsymbol{\Xi}^{\alpha} : \mathbf{d} - \sum\limits_{\beta=1}^{n} M_{\alpha\beta}\overset{\bullet}{\gamma}^{\beta}\right) n^{\alpha} = 0 \quad \text{for} \quad \overset{\bullet}{\gamma}^{\alpha} \neq 0 \\ \left(\boldsymbol{\Xi}^{\alpha} : \bar{\mathbf{d}} - \sum\limits_{\beta=1}^{n} M_{\alpha\beta}\overset{\bullet}{\bar{\gamma}}^{\beta}\right) n^{\alpha} = 0 \quad \text{for} \quad \overset{\bullet}{\bar{\gamma}}^{\alpha} \neq 0 \end{array}\right\} \tag{19.70}$$

which leads to

$$\boldsymbol{\Xi}^{\alpha} : \Delta\mathbf{d} - \sum_{\beta=1}^{n} M_{\alpha\beta}\Delta\dot{\gamma}^{\beta} = 0 \tag{19.71}$$

where $\Delta\mathbf{d} \equiv \mathbf{d} - \bar{\mathbf{d}}$ and $\Delta\dot{\gamma}^{\beta} \equiv \dot{\gamma}^{\beta} - \dot{\bar{\gamma}}^{\beta}$. Multiplying $\Delta\dot{\gamma}^{\alpha}$ to Eq. (19.71), we have

$$\boldsymbol{\Xi}^{\alpha} : \Delta\mathbf{d}\Delta\dot{\gamma}^{\alpha} = \sum_{\beta=1}^{n} M_{\alpha\beta}\Delta\dot{\gamma}^{\beta}\Delta\dot{\gamma}^{\alpha} \tag{19.72}$$

Next, we assume that the slip system α is active in the first mode but it is inactive in the second mode, i.e. $\dot{\gamma}^{\alpha} \neq 0$, $\dot{\bar{\gamma}}^{\alpha} = 0$, so that

$$\left.\begin{array}{ll} \left(\boldsymbol{\Xi}^{\alpha} : \mathbf{d} - \sum\limits_{\beta=1}^{n} M_{\alpha\beta}\dot{\gamma}^{\beta}\right) n^{\alpha} = 0 & \text{for} \quad \dot{\gamma}^{\alpha} \neq 0 \\ \left(\boldsymbol{\Xi}^{\alpha} : \bar{\mathbf{d}} - \sum\limits_{\beta=1}^{n} M_{\alpha\beta}\dot{\bar{\gamma}}^{\beta}\right) n^{\alpha} < 0 & \text{for} \quad \dot{\bar{\gamma}}^{\alpha} = 0 \end{array}\right\} \tag{19.73}$$

which leads to

$$\left(\boldsymbol{\Xi}^{\alpha} : \Delta\mathbf{d} - \sum_{\beta=1}^{n} M_{\alpha\beta}\Delta\dot{\gamma}^{\beta}\right) n^{\alpha} > 0 \tag{19.74}$$

Noting

$$n^{\alpha}\Delta\dot{\gamma}^{\alpha} = n^{\alpha}\dot{\gamma}^{\alpha} > 0$$

Equation (19.74) leads to

$$\left(\boldsymbol{\Xi}^{\alpha} : \Delta\mathbf{d} - \sum_{\beta=1}^{n} M_{\alpha\beta}\Delta\dot{\gamma}^{\beta}\right) n^{\alpha} n^{\alpha}\Delta\dot{\gamma}^{\alpha} > 0$$

from which it follows that

$$\boldsymbol{\Xi}^{\alpha} : \Delta\mathbf{d}\Delta\dot{\gamma}^{\alpha} > \sum_{\beta=1}^{n} M_{\alpha\beta}\Delta\dot{\gamma}^{\beta}\Delta\dot{\gamma}^{\alpha} \tag{19.75}$$

Consider the inverse case that the slip system α is inactive in the first mode and active in the second mode, i.e. $\dot{\gamma}^{\alpha} = 0$, $\dot{\bar{\gamma}}^{\alpha} \neq 0$, so that

$$\left.\begin{aligned} (\boldsymbol{\Xi}^\alpha : \mathbf{d} - \sum_{\beta=1}^{n} M_{\alpha\beta}\overset{\bullet}{\gamma}^\beta)n^\alpha < 0 \quad \text{for} \quad \overset{\bullet}{\gamma}^\alpha = 0 \\ (\boldsymbol{\Xi}^\alpha : \mathbf{d} - \sum_{\beta=1}^{n} M_{\alpha\beta}\overset{\bullet}{\gamma}^\beta)n^\alpha = 0 \quad \text{for} \quad \overset{\bullet}{\bar{\gamma}}^\alpha \neq 0 \end{aligned}\right\} \tag{19.76}$$

from which it follows that

$$\left(\boldsymbol{\Xi}^\alpha : \Delta\mathbf{d} - \sum_{\beta=1}^{n} M_{\alpha\beta}\Delta\overset{\bullet}{\gamma}^\beta\right)n^\alpha < 0$$

for which, noting

$$n^\alpha \Delta\overset{\bullet}{\gamma}^\alpha = -n^\alpha \overset{\bullet}{\bar{\gamma}}^\alpha < 0$$

it follows that

$$\left(\boldsymbol{\Xi}^\alpha : \Delta\mathbf{d} - \sum_{\beta=1}^{n} M_{\alpha\beta}\Delta\overset{\bullet}{\gamma}^\beta\right)n^\alpha n^\alpha \Delta\overset{\bullet}{\gamma}^\alpha > 0$$

Consequently, the inequality in Eq. (19.75) holds also in this case.

Furthermore, in the case that the slip system α is inactive in both of the first and the second modes, i.e. $\overset{\bullet}{\gamma}^\alpha = 0, \overset{\bullet}{\bar{\gamma}}^\alpha = 0$ leading to $\Delta\overset{\bullet}{\gamma}^\alpha = 0$, so that the equality in Eq. (19.72) holds. Consequently, the following inequality holds in all the above-mentioned four cases.

$$\boldsymbol{\Xi}^\alpha : \Delta\mathbf{d}\Delta\overset{\bullet}{\gamma}^\alpha \geq \sum_{\beta=1}^{n} M_{\alpha\beta}\Delta\overset{\bullet}{\gamma}^\beta \Delta\overset{\bullet}{\gamma}^\alpha \tag{19.77}$$

Taking the total sum of Eq. (19.77) for all of slip systems, the following inequality holds.

$$\sum_{\alpha=1}^{n} \boldsymbol{\Xi}^\alpha : \Delta\mathbf{d}\Delta\overset{\bullet}{\gamma}^\alpha \geq \sum_{\alpha=1}^{n}\sum_{\beta=1}^{n} M_{\alpha\beta}\Delta\overset{\bullet}{\gamma}^\beta \Delta\overset{\bullet}{\gamma}^\alpha \tag{19.78}$$

$\Delta\mathbf{d} = \mathbf{O}$ holds for given strain rate, and if $M_{\alpha\beta}$ is the positive-definite matrix, the right-hand side in Eq. (19.78) is non-negative, so that the uniqueness of slip mode, i.e. $\Delta\overset{\bullet}{\gamma}^\alpha = 0$ holds. In other words, $M_{\alpha\beta}$ must be positive-definite in order that the uniqueness of slip mode, i.e. the uniqueness of $\overset{\bullet}{\gamma}^\alpha$ holds for given strain rate $\mathbf{d}$. Then, the matrix $M_{\alpha\beta}$ is called the effective slip-systems hardening moduli. The matrix $M_{\alpha\beta}$ is asymmetric, i.e. $M_{\alpha\beta} \neq M_{\beta\alpha}$ and thus it is not the positive-definite matrix, so that the uniqueness of slip mode does not holds in general.

The uniqueness of the matrix $M_{\alpha\beta}$ depends on the hardening coefficient, state of stress and the number and the directions of critical shear stress sensitively. It is not guaranteed and its tendency is remarkable for a higher latent hardening (Hill 1966; Hill and Rice 1972; Havner 1982; Asaro 1983; Franciosi and Zaoli 1991).

19.7 Various Schemes for Calculation of Shear Strain Rates

Big time is required for calculating shear strain rates in numerous slip systems. Then, various schemes for the improvement of the calculation have been proposed to date. Main schemes for the improvement will be explained in this section.

19.7.1 Singular Value Decomposition

It is required to solve Eq. (19.57) in order to calculate shear strain rates in slip systems directly from macroscopic strain rate applied to crystalline. However, the matrix $M_{\alpha\beta}$ is not positive-definite, so that there does not exist a unique solution in general as described in the last section. The *singular value decomposition* is used to calculate the solution with the shortest path (Golub and Van Loan 2013; Press et al. 1988). It has been applied to the crystal plasticity by Anand and Kothari (1996) and used widely by Miehe and Schroder (2001), Knockaert et al. (2000), Yoshida and Kuroda (2012), etc. The singular value decomposition is explained in this subsection.

The general second-order tensor $\mathbf{T}$ in the n-dimensional space which is asymmetric and thus cannot be led to the spectral decomposition in general. On the other hand, designating the eigenvectors of the positive-definite tensors $\mathbf{T}\mathbf{T}^T$ and $\mathbf{T}^T\mathbf{T}$ as $\mathbf{u}_\rho$ and $\mathbf{v}_\rho$ $(\rho = 1, 2, \cdots, n)$, respectively, and their eigenvalues σ_ρ^2 because they are positive, it follows that

$$\left.\begin{aligned}\mathbf{T}\mathbf{T}^T &= \sum_{\rho=1}^{n} \sigma_\rho^2 \mathbf{u}_\rho \otimes \mathbf{u}_\rho \\ \mathbf{T}^T\mathbf{T} &= \sum_{\rho=1}^{n} \sigma_\rho^2 \mathbf{v}_\rho \otimes \mathbf{v}_\rho\end{aligned}\right\} \tag{19.79}$$

i.e.

$$\left.\begin{aligned}\mathbf{T}\mathbf{T}^T\mathbf{u}_\rho &= \sigma_\rho^2 \mathbf{u}_\rho \\ \mathbf{T}^T\mathbf{T}\mathbf{v}_\rho &= \sigma_\rho^2 \mathbf{v}_\rho\end{aligned}\right\} \tag{19.80}$$

while $\mathbf{u}_\rho$, $\mathbf{v}_\rho$ and σ_ρ are not the eigenvectors and eigenvalues except for the symmetric tensor $\mathbf{T}$.

Exploiting the eigen values and vectors defined above, the tensor $\mathbf{T}$ can be led to the following singular value decomposition.

$$\mathbf{T} = \mathbf{U}\boldsymbol{\Sigma}\mathbf{V}^T \tag{19.81}$$

where $\boldsymbol{\Sigma}$ is the diagonalized tensor with the components $\sigma_1, \sigma_2, \cdots, \sigma_n$ and thus it is described as follows:

$$\boldsymbol{\Sigma} = \mathrm{diag}(\sigma_1,\ \sigma_2,\ \cdots,\ \sigma_n) = \begin{bmatrix} \sigma_1 & 0 & \cdots & 0 \\ 0 & \sigma_2 & \cdots & 0 \\ \vdots & \vdots & \ddots & \vdots \\ 0 & 0 & \cdots & \sigma_n \end{bmatrix} \tag{19.82}$$

provided that the order of the magnitudes of these components is $\sigma_1 \geq \sigma_2 \geq \cdots \geq \sigma_n (\geq 0)$. $\mathbf{U}$ and $\mathbf{V}$ are the orthogonal tensors by lining the eigenvectors in column (horizontally).

$$\left.\begin{aligned} \mathbf{U} &= \lfloor \mathbf{u}_1\ \mathbf{u}_2 \cdots \mathbf{u}_n \rfloor = \begin{Bmatrix} \mathbf{u}_1 \\ \mathbf{u}_2 \\ \vdots \\ \mathbf{u}_n \end{Bmatrix} = \begin{bmatrix} u_{11} & u_{12} & \cdots & u_{1n} \\ u_{21} & u_{22} & \cdots & u_{2n} \\ \vdots & \vdots & \ddots & \vdots \\ u_{n1} & u_{n2} & \cdots & u_{nn} \end{bmatrix} \\ \mathbf{V} &= \lfloor \mathbf{v}_1\ \mathbf{v}_2 \cdots \mathbf{v}_n \rfloor = \begin{Bmatrix} \mathbf{v}_1 \\ \mathbf{v}_2 \\ \vdots \\ \mathbf{v}_n \end{Bmatrix} = \begin{bmatrix} v_{11} & v_{12} & \cdots & v_{1n} \\ v_{21} & v_{22} & \cdots & v_{2n} \\ \vdots & \vdots & \ddots & \vdots \\ v_{n1} & v_{n2} & \cdots & v_{nn} \end{bmatrix} \end{aligned}\right\} \tag{19.83}$$

where the components of each vector are lined up in row (vertically), satisfying

$$\mathbf{U}\mathbf{U}^T = \mathbf{U}^T\mathbf{U} = \mathbf{V}\mathbf{V}^T = \mathbf{V}^T\mathbf{V} = \mathbf{I}\,(||\mathbf{U}|| = ||\mathbf{V}|| = 1) \tag{19.84}$$

noting $(\mathbf{U}\mathbf{U}^T)_{ij} = U_{ir}U_{jr} = (\mathbf{u}_i \cdot \mathbf{e}_r)(\mathbf{u}_j \cdot \mathbf{e}_r) = \mathbf{u}_i \cdot (\mathbf{u}_j \cdot \mathbf{e}_r)\mathbf{e}_r = \mathbf{u}_i \cdot \mathbf{u}_j = \delta_{ij}$. It follows from Eqs. (19.81) and (19.84) that

$$\left.\begin{aligned} \mathbf{T}\mathbf{T}^T &= \mathbf{U}\boldsymbol{\Sigma}\mathbf{V}^T\mathbf{V}\boldsymbol{\Sigma}\mathbf{U}^T = \mathbf{U}\boldsymbol{\Sigma}^2\mathbf{U}^T \\ \mathbf{T}^T\mathbf{T} &= \mathbf{V}\boldsymbol{\Sigma}\mathbf{U}^T\mathbf{U}\boldsymbol{\Sigma}\mathbf{V}^T = \mathbf{V}\boldsymbol{\Sigma}^2\mathbf{V}^T \end{aligned}\right\} \tag{19.85}$$

The pseudo-inverse tensor $\mathbf{T}^\dagger$ of $\mathbf{T}$ is defined by

$$\mathbf{T}^\dagger \equiv \mathbf{V}\boldsymbol{\Sigma}^\dagger\mathbf{U}^T \tag{19.86}$$

where

$$\boldsymbol{\Sigma}^\dagger = \mathrm{diag}(1/\sigma_1,\ 1/\sigma_2,\ \cdots 1/\sigma_r,\ 0\cdots 0) = \begin{bmatrix} \sigma_1^{-1} & 0\cdots & 0 & 0\cdots 0 \\ 0 & \sigma_2^{-1}\cdots & 0 & 0\cdots 0 \\ \vdots & \vdots\ \ddots & \vdots & \vdots \\ 0 & 0\cdots & \sigma_r^{-1} & 0\cdots 0 \\ 0 & 0\cdots & 0 & 0\cdots 0 \\ \vdots & \vdots & \vdots & \vdots\ \ddots\ \vdots \\ 0 & 0\cdots & 0 & 0\cdots 0 \end{bmatrix} \tag{19.87}$$

provided that we set $1/\sigma_i = 0\ (i = 1, 2, \ldots, r)$ for $\sigma_i = 0\ (i = r + 1, 2, \ldots, n)$, obviously fulfilling $\boldsymbol{\Sigma}\boldsymbol{\Sigma}^\dagger = \mathbf{I}$. It is confirmed that the following equation holds from Eqs. (19.81), (19.84) and (19.86).

$$\mathbf{T}\mathbf{T}^\dagger = \mathbf{U}\boldsymbol{\Sigma}\mathbf{V}^T\mathbf{V}\boldsymbol{\Sigma}^\dagger\mathbf{U}^T = \mathbf{I} \tag{19.88}$$

Consider the following tensor equation with the vectors $\mathbf{x}$ and $\mathbf{c}$.

$$\mathbf{T}\mathbf{x} = \mathbf{c} \tag{19.89}$$

If $\mathbf{T}$ is the singular tensor, there exist numerous solutions for $\mathbf{x}$. The vector $\mathbf{x}$ is expressed noting Eqs. (19.86) and (19.88) as follows:

$$\mathbf{x} = \mathbf{T}^\dagger\mathbf{c} = \mathbf{V}\boldsymbol{\Sigma}^\dagger\mathbf{U}^T\mathbf{c} = \mathbf{V}\mathrm{dia}(1/\sigma_j)\mathbf{U}^T\mathbf{c} \tag{19.90}$$

which is called the *singular value decomposition* and calculated from the right to the left. The solution obtained by the singular value decomposition is unique and possesses the shortest path among numerous solutions satisfying the original equation as will be proved as follows.

There exists the zero-dimensional subspace of the vector $\mathbf{x}$ projected to zero vector if $\mathbf{T}$ is the singular tensor. Designating the solution of Eq. (19.90) for an arbitrary tensor $\boldsymbol{\Sigma}^\dagger$ possessing non-zero component only in the zero component in Eq. (18.87) by $\mathbf{x}'$, it follows for the vector $\mathbf{x} + \mathbf{x}'$ noting Eqs. (19.86) and (19.90) that

$$\begin{aligned}||\mathbf{x}+\mathbf{x}'|| &= ||\mathbf{T}^{\dagger}\mathbf{c}+\mathbf{x}'|| = ||\mathbf{V}\boldsymbol{\Sigma}^{\dagger}\mathbf{U}^{T}\mathbf{c}+\mathbf{x}'|| \\ &= ||\mathbf{V}(\boldsymbol{\Sigma}^{\dagger}\mathbf{U}^{T}\mathbf{c}+\mathbf{V}^{T}\mathbf{x}')|| = ||\mathbf{V}||\,||\boldsymbol{\Sigma}^{\dagger}\mathbf{U}^{T}\mathbf{c}+\mathbf{V}^{T}\mathbf{x}'|| \\ &= ||\boldsymbol{\Sigma}^{\dagger}\mathbf{U}^{T}\mathbf{c}+\mathbf{V}^{T}\mathbf{x}'||\end{aligned} \tag{19.91}$$

The components in the second term are non-zero in the zero components in the first terms and they are orthogonal and thus independent to each other in the n-dimensional orthogonal coordinate system, so that the minimum of the quantity in Eq. (19.91) holds for $\mathbf{x}' = \mathbf{0}$ leading to the vector $\mathbf{x}$ as the singular value decomposition.

Consider the following tensor based on the above-mentioned singular value decomposition.

$$\overline{\mathbf{T}} = (\mathbf{T} + \varepsilon\mathbf{I}) \tag{19.92}$$

where $\overline{\mathbf{T}}$ is the nonsingular tensor made by adding the infinitesimal perturbation tensor $\varepsilon\mathbf{I}$ to the singular tensor $\mathbf{T}$. Adopting it in Eq. (19.89), we have

$$\mathbf{x} = (\mathbf{T} + \varepsilon\mathbf{I})^{-1}\mathbf{c} \tag{19.93}$$

from which we can obtain the similar solution to that due to the singular value decomposition. This is the simplest solution of the singular equation and called the *diagonal shift method* (Miehe and Schroder 2001).

Number of unknown quantities on shear strain rates is larger than nine given equations on macroscopic strain rate components in the crystal plasticity, so that solution is not determined uniquely. In such case, we may solve by supplementing the lines composed of zero components to the matrix $\mathbf{T}$ and the zero components to the vector $\mathbf{c}$ for the difference of numbers in unknown quantities and given equations. By applying the singular value decomposition to the simultaneous equation made by this method, we can obtain the solution with the shortest path. It corresponds to the minimum shear principle by Taylor (1938).

19.7.2 Regularized Schmid Law

The yield surface in the slip systems is formed by plural intersecting planes in the stress space so that it possesses the sharp corner. Then, the shear strain rates must be calculated in each slip systems. In order to avoid this complicated work, the *regularized Schmid law* has been studied, in which the yield surface with rounded-off corners is formulated and the only one plastic multiplier by applying the associated flow rule to that yield surface is calculated.

The yield condition in slip system is described by

$$\frac{|\tau^{\alpha}|}{\tau_{y}^{\alpha}} - 1 = 0 \qquad (19.94)$$

The slip systems described by Eq. (19.94) give rise to the yield surfaces composed of the planes in number of slip systems, exhibiting the sharp corners at their intersections. A single smooth yield surface can be formulated by smoothing the envelope of the yield surfaces in Eq. (19.94) (Gambin 1991, 2001; Gambin and Barlat 1997; Darrieulat and Piot 1996; Zamiri et al. 2007; Zamiri and Pourboghrat 2010). This is regarded as the invocation of the method to derive the Mises yield surface from the Tresca yield condition by Hosford (1974, 2009). Zamiri et al. (2007) proposed the following simple yield surface.

$$f = \left(\sum_{\alpha=1}^{n} \frac{\tau^{\alpha}}{\tau_{y}^{\alpha}} \left| \frac{\tau^{\alpha}}{\tau_{y}^{\alpha}} \right|^{2n-1} - 1 \right)^{1/m} = \left(\sum_{\alpha=1}^{n} \frac{\tau^{\alpha}}{\tau_{y}^{\alpha}} \left| \frac{\mathbf{p}^{\alpha} : \boldsymbol{\tau}}{\tau_{y}^{\alpha}} \right|^{2n-1} - 1 \right)^{1/m} = 0 \qquad (19.95)$$

noting Eq. (19.27). $m(\geq 1)$ is the material constant for smoothing the corner of yield surface, while the larger m is, the smoother the yield surface is. While Eq. (19.95) is of the power form, in order to avoid the problem on the numerical calculation caused by the power function, Zamiri and Pourboghrat (2010) proposed the yield surface in the logarithm-exponential function.

$$f = \frac{1}{\rho} \ln \left\{ \sum_{\alpha=1}^{n} \exp \left[\rho \left(\left| \frac{\mathbf{p}^{\alpha} : \boldsymbol{\tau}}{\tau_{y}^{\alpha}} \right| - 1 \right) \right] \right\} = 0 \qquad (19.96)$$

where $\rho\,(\geq 1)$ is the material constant for smoothing the corner of yield surface, while the larger ρ is, the smoother the yield surface is.

The plastic strain rate for the above-mentioned yield condition with the associated flow rule is given by

$$\mathbf{d}^{p} = \dot{\lambda} \frac{\partial f}{\partial \boldsymbol{\tau}} \, (\dot{\lambda} \geq 0) \qquad (19.97)$$

The plastic multiplier $\dot{\lambda}$ is calculated by the formulation based on the consistency condition of the yield condition (Gambin 1997, 2001; Gambin and Barlat 1997) or the return-mapping (Zamiri et al. 2007; Zamiri and Pourboghrat 2010).

The above-mentioned regularized Schmid law reduces the calculation time since only one plastic multiplier for the single yield surface has only to be calculated. However, it would deviate from the primary purpose of the crystal plasticity for deriving the macroscopic behavior from the microscopic physical law, since it replaces the yield conditions in multi slip systems to the global yield surface.

19.7.3 Creep-Type Crystal Plasticity Mode

The crystal elastoplastic constitutive equation described in the last section possesses the difficulties:

(1) The yield judgment whether the resolved shear stresses τ^α reach the critical shear stress τ_y^α is required.
(2) Particular algorithm to pull-back the resolved shear stresses to the critical shear stress must be incorporated.

These procedures must be executed in numerous slip systems and thus the analysis by this constitutive equation is so complicated as actually impossible. Then, the crystal plasticity analyses by the creep model is widely used as will be described below.

Nakada and Keh (1966) first advocated and ten years later Hutchinson (1976) presented the following creep-type rate-dependent equation of crystalline slip rate, which are widely adopted after the review report by Peirce et al. (1982, 1983) for single crystals and Asaro and Needleman (1985) for polycrystal.

$$\dot{\gamma}^{c\alpha} = \dot{\gamma}_0{}^{c\alpha} \left(\frac{\tau^\alpha}{\tau_y^\alpha} \right) \left| \frac{\tau^\alpha}{\tau_y^\alpha} \right|^{(1/m)-1} \tag{19.98}$$

where $\dot{\gamma}_0^{c\alpha}$ is the reference rate of shearing which is taken usually same in all slip systems and m is the material constant, while for $m < 0.02$ the creep slip rate $\dot{\gamma}^{c\alpha}$ is induced abruptly when the magnitude of shear stress, $|\tau^\alpha|$, reaches the shear-yield stress τ_y^α. All the slip systems are active and thus the selection of active ones is not required for Eq. (19.98). However, Eq. (19.98) possesses the following fundamental impertinences.

(1) It depends only on the shear stress because it falls within the framework of the creep-type viscoplasticity. Therefore, the creep crystalline slip rate is determined only by the current shear stress with time and thus an arbitrary deformation rate cannot be given to the material obeying Eq. (19.98) which is independent of the stress rate as far as a large elastic deformation of crystal lattice is not incorporated. In other words, it cannot be applied to rigid-viscoplastic materials. In facts, however, the crystalline slip rate would have to depend not only on the shear stress but also on its rate in a quasi-static deformation at room temperature. On the other hand, the rate-independent equation of plastic slip rate $\dot{\gamma}^{p\alpha}$ must depend on both the shear stress and its rate (magnitude) in the slip system because it falls within the framework of the plasticity.
(2) It belongs to the creep type model without a definite yield stress among the viscoplastic models. Therefore, it predicts always the creep deformation except for the stress-free state, and thus the creep slip rate is induced even when the magnitude of shear stress, $|\tau^\alpha|$, decreases as illustrated in Fig. 19.3 in which a

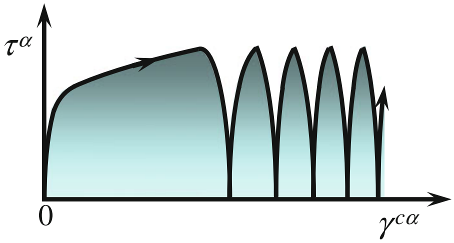

Fig. 19.3 Shear stress versus crystalline slip curves accompanied with excessive mechanical ratcheting predicted by creep model (Peirce et al. 1983)

general trend is intelligibly shown for a moderate value of m. It is unrealistic as known from the fact that any metallic solid has never collapsed under their own weight at room temperature as indicated in p. 201 in Havner (1992). Needless to say, it cannot be applied to the description of cyclic loading behavior since it does not possess a loading criterion and thus it predicts identical deformation behavior in the reloading process and in the unloading process. Therefore, it predicts excessively large mechanical ratcheting as illustrated in Fig. 19.3. In general, the viscoplastic deformation behavior cannot be described pertinently by the creep-type model and instead it can be predicted realistically by the overstress-type model possessing the loading criterion as explained in Sect. 13.3.

As examined above, the creep-type equation of crystalline slip contains fundamental defects. Then, it has been the strong desire over the last half century to find the physically and numerically pertinent rate-independent equation of crystalline slip rate. This fact is declared emotionally as "*The various viscoplastic, finite-strain aggregate calculations reviewed in this section, and similar ones in the literature, are computationally impressive (although which approximate polycrystal model is superior appears to be an open question). However, one hopes that there may soon evolve a theory of rate-dependent crystalline slip in metals that would leave such great structural landmarks as the Eiffel Tower, Empire State Building, and Golden Gate Bridge still standing*" in p. 204 of Havner (1992). The landmark would have been found in the subloading crystal plasticity model described in the next section, while it is not a rate-dependent formulation but is a rate-independent formulation falling within the framework of plasticity based on the subloading surface concept.

All of the afore-mentioned defects in the rate-dependent crystalline slip rate are dissolved by subloading crystal plasticity model. The crucial importance for the incorporation of the subloading concept is manifested most distinctly in the crystal plasticity analysis which is required to calculate slips in numerous number of slip systems, while the yield judgment is not required and the stress is automatically attracted to the yield surface only in the subloading crystal plasticity model.

19.8 Subloading Crystal Plasticity Model

The crystal shear yield condition describing the *crystal shear yield region* in the slip system α is given by

$$|\hat{\tau}^{\alpha}| = \tau_y^{\alpha} \tag{19.99}$$

where

$$\hat{\tau}^{\alpha} \equiv \tau^{\alpha} - \chi^{\alpha} \tag{19.100}$$

χ^{α} is the shear kinematic hardening variable and $\tau_y^{\alpha}\,(>0)$ is the shear hardening function, referred to as the *critical shear stress*, in the slip system α.

Now, incorporate the shear subloading region described by the following relation based on the subloading concept (Hashiguchi 2015).

$$|\hat{\tau}^{\alpha}| = r^{\alpha}\tau_y^{\alpha}, \text{ i.e.} r^{\alpha} \equiv \frac{|\hat{\tau}^{\alpha}|}{\tau_y^{\alpha}} \tag{19.101}$$

where $r^{\alpha}(0 \le r^{\alpha} \le 1)$ is referred to as the *normal-yield shear ratio* which designates always the ratio of $|\tau^{\alpha} - \chi^{\alpha}|$ to the critical shear stress τ_y^{α} not only in the slipping process $(\overset{\bullet}{\gamma}{}^{p\alpha} \neq 0)$ but also in the non-slipping process $(\overset{\bullet}{\gamma}{}^{p\alpha} = 0)$.

The associated flow rule to the subloading shear region is adopted for the plastic shear strain rate as follows:

$$\overset{\bullet}{\gamma}{}^{p\alpha} = \overset{\bullet}{\lambda}{}^{\alpha}\hat{n}^{\alpha}\ (\overset{\bullet}{\lambda}{}^{\alpha} \ge 0)\ (|\overset{\bullet}{\gamma}{}^{p\alpha}| = \overset{\bullet}{\lambda}{}^{\alpha}) \tag{19.102}$$

The material-time derivative of Eq. (19.101) reads:

$$\hat{n}^{\alpha}(\overset{\bullet}{\tau}{}^{\alpha} - \overset{\bullet}{\chi}{}^{\alpha}) = r^{\alpha}\overset{\bullet}{\tau}_y{}^{\alpha} + \overset{\bullet}{r}{}^{\alpha}\tau_y^{\alpha} \tag{19.103}$$

i.e.

$$\overset{\bullet}{\tau}{}^{\alpha} = \hat{n}^{\alpha}r^{\alpha}\overset{\bullet}{\tau}_y{}^{\alpha} + \overset{\bullet}{\chi}{}^{\alpha} + \hat{n}^{\alpha}\overset{\bullet}{r}{}^{\alpha}\tau_y^{\alpha} \tag{19.104}$$

The rate of critical shear stress is specified by

$$\overset{\bullet}{\tau}_y{}^{\alpha} = \sum_{\beta=1}^{n} h_{\alpha\beta}|\overset{\bullet}{\gamma}{}^{p\beta}| = \sum_{\beta=1}^{n} h_{\alpha\beta}\overset{\bullet}{\lambda}{}^{\beta} \tag{19.105}$$

where $h_{\alpha\beta}$ is given by the following matrix which is the function of the plastic shear strain (Peirce et al. 1982).

$$h_{\alpha\beta} = qh(\gamma^p) + (1-q)h(\gamma^p)\delta_{\alpha\beta}(= h_{\beta\alpha}) = \begin{cases} h(\gamma^p) & \text{for } i = j \\ qh(\gamma^p) & \text{for } i \neq j \end{cases} (1 \leq q \leq 1.4) \tag{19.106}$$

$h(\gamma^p)$ is given by the functional form

$$h(\gamma^p) = h_0 \mathrm{sech}^2\left(\frac{h_0\gamma^p}{\tau_s - \tau_{y0}}\right) \tag{19.107}$$

with

$$\gamma^p \equiv \sum_{\beta=1}^{n} \int_0^t |\dot{\gamma}^{p\beta}| dt \tag{19.108}$$

h_0 and τ_{y0} are the initial values of h and τ_y^α, i.e. $h_0 = h(0)$ and $\tau_{y0} = \tau_y^\alpha(0)$, respectively, and τ_s is the saturation value of τ_y^α, i.e. $\tau_s = \tau_y^\alpha(\infty)$.

Assume the following shear nonlinear-kinematic hardening rule.

$$\dot{\chi}^\alpha = c_\chi\left(\dot{\gamma}^{p\alpha} - \frac{1}{\zeta_\chi\tau_y^\alpha}|\dot{\gamma}^{p\alpha}|\chi^\alpha\right) = c_\chi\dot{\lambda}^\alpha\left(\hat{n}^\alpha - \frac{1}{\zeta_\chi\tau_y^\alpha}\chi^\alpha\right) \tag{19.109}$$

where c_χ and ζ_χ are the material constants. The latent hardening may be incorporated for the shear kinematic hardening (e.g. Bassani and Wu 1991; Harder 1999; Xu and Jiang 2004).

Referring to the Sect. 7.2 on the subloading surface model, let us postulate for the crystalline shear strain rate as follows: *The crystalline plastic shear strain rate is induced when the resolved stress approaches the critical shear stress but only the crystalline elastic shear strain rate is induced when the resolved stress lowers from the critical shear stress*, while the resolved stress rate causes the crystalline elastic shear strain rate inevitably. In other words, **the resolved shear stress approaches the critical shear stress when a crystalline plastic shear strain rate is induced but it lowers from the critical shear stress when only a crystalline elastic shear strain rate occurs**. Here, note that the approaching degree to the resolved shear stress to the critical shear stress is described by the shear normal-yield ratio R^α. Then, let the evolution equation of shear normal-yield ratio r^α be given analogously to Eq. (7.9) for the normal-yield ratio R of the subloading surface model as follows:

$$\dot{r}^\alpha = U(r^\alpha)|\dot{\gamma}^{p\alpha}| = U(r^\alpha)\dot{\lambda}^\alpha \quad \text{for} \quad \dot{\gamma}^{p\alpha} \neq 0 \tag{19.110}$$

where the function $U(r^\alpha)$ fulfills the conditions (see Fig. 19.4):

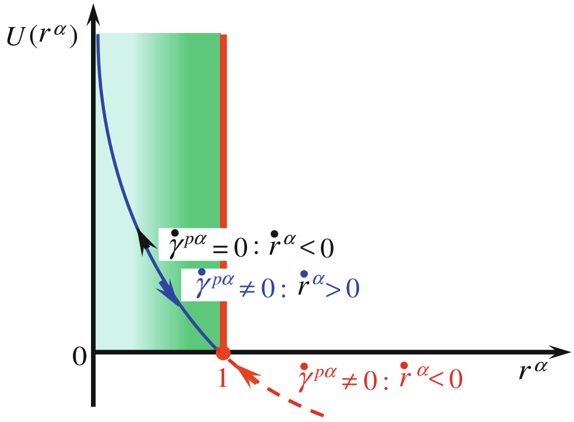

Fig. 19.4 Function $U(r^\alpha)$ in the evolution rule of shear normal-yield ratio R^α

$$U(r^\alpha)\begin{cases} \to +\infty & \text{for} \quad r^\alpha = 0 \text{ (elastic state)} \\ > 0 & \text{for} \quad 0 < r^\alpha < 1 \text{ (subyield state)} \\ = 0 & \text{for} \quad r^\alpha = 1 \text{ (normal-yield state)} \\ < 0 & \text{for} \quad r^\alpha > 1 \text{ (over normal-yield state)} \end{cases} \tag{19.111}$$

Let the explicit function of $U(r^\alpha)$ be given by

$$U(r^\alpha) = u_c \cot[(\pi/2) r^{\alpha^{n_c}}] \tag{19.112}$$

where u_c and $n_c(\geq 1)$ are the material constants.

The smooth shear stress versus crystalline shear strain curve is depicted and the resolved shear stress is automatically attracted to the critical shear stress because of $\dot{r}^\alpha < 0$ for $r^\alpha > 1$ (over shear normal-yield state) in Eq. (19.110) with Eq. $(19.111)_4$ as shown in Fig. 19.5.

Substituting Eqs. (19.105), (19.109) and (19.110) into Eq. (19.103), one has the consistency condition for the subloading crystalline shear region.

$$\dot{\tau}^\alpha = \hat{n}^\alpha r^\alpha \sum_{\beta=1}^{n} h_{\alpha\beta} \dot{\lambda}^\beta + c_\chi \left(\hat{n}^\alpha - \frac{1}{\zeta_\chi \tau_y^\alpha} \chi^\alpha \right) \dot{\lambda}^\alpha + \hat{n}^\alpha U(r^\alpha) \tau_y^\alpha \dot{\lambda}^\alpha \tag{19.113}$$

from which it follows that

$$\dot{\tau}^\alpha = \sum_{\beta=1}^{n} \bar{h}_{\alpha\beta} \dot{\lambda}^\beta \tag{19.114}$$

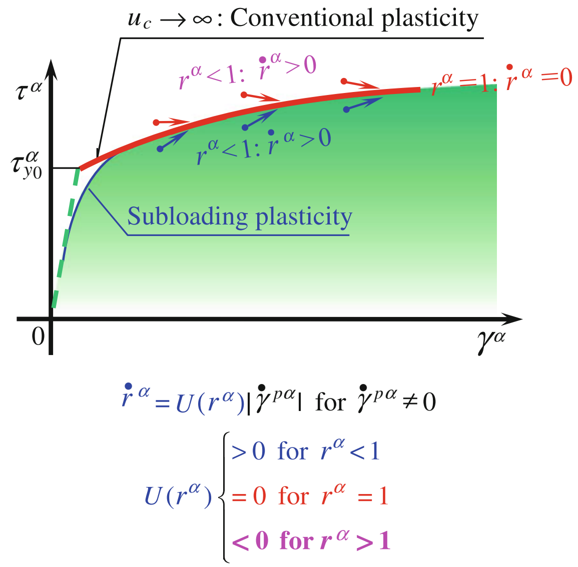

Fig. 19.5 Resolved shear stress is automatically attracted to critical shear stress in plastic shear process

where

$$\bar{h}_{\alpha\beta} \equiv \hat{n}^\alpha r^\alpha h_{\alpha\beta} + c_\chi \left(\hat{n}^\alpha - \frac{1}{\zeta_\chi \tau_y^\alpha} \chi^\alpha \right) \delta_{\alpha\beta} + \hat{n}^\alpha U(r^\alpha) \tau_y^\alpha \delta_{\alpha\beta} \; (\neq \bar{h}_{\beta\alpha}) \tag{19.115}$$

Equating Eq. (19.32) with (19.114), it follows that

$$\boldsymbol{\Xi}^\alpha : \left(\mathbf{d} - \sum_{\beta=1}^{n} \mathbf{p}^\beta \hat{n}^\beta \dot{\lambda}^\beta \right) = \sum_{\beta=1}^{n} \bar{h}_{\alpha\beta} \dot{\lambda}^\beta \tag{19.116}$$

which is rewritten as

$$\boldsymbol{\Xi}^\alpha : \mathbf{d} = \sum_{\beta=1}^{n} \overline{M}_{\alpha\beta} \dot{\lambda}^\beta \tag{19.117}$$

where

$$\overline{M}_{\alpha\beta} \equiv \bar{h}_{\alpha\beta} + \boldsymbol{\Xi}^\alpha : \mathbf{p}^\beta \hat{n}^\beta \; (\neq \overline{M}_{\beta\alpha}) \tag{19.118}$$

The plastic shear strain rate is given from Eq. (19.117) as follows:

$$\dot{\lambda}^{\alpha} = \sum_{\beta=1}^{n} \overline{M}_{\alpha\beta}^{-1} \boldsymbol{\Xi}^{\beta} : \mathbf{d} \tag{19.119}$$

Substituting Eq. (19.119) into Eq. (19.54), it follows that

$$\overset{\circ}{\boldsymbol{\tau}}{}^{w} = \mathbf{E} : \mathbf{d} - \sum_{\alpha=1}^{n} \boldsymbol{\Xi}^{\alpha} \dot{\lambda}^{\alpha} \hat{n}^{\alpha} = \mathbf{E} : \mathbf{d} - \sum_{\alpha=1}^{n} \boldsymbol{\Xi}^{\alpha} \hat{n}^{\alpha} \sum_{\beta=1}^{n} \overline{M}_{\alpha\beta}^{-1} \boldsymbol{\Xi}^{\beta} : \mathbf{d}$$

leading to

$$\overset{\circ}{\boldsymbol{\tau}}{}^{w} = \overline{\mathbf{K}}^{ep} : \mathbf{d} \tag{19.120}$$

where

$$\overline{\mathbf{K}}^{ep} \equiv \mathbf{E} - \sum_{\alpha=1}^{n} \sum_{\beta=1}^{n} \boldsymbol{\Xi}^{\alpha} \otimes \hat{n}^{\alpha} \overline{M}_{\alpha\beta}^{-1} \boldsymbol{\Xi}^{\beta} \; (\neq \overline{\mathbf{K}}^{epT}) \tag{19.121}$$

The loading criterion for the plastic shear strain rate is given by the sign of the plastic multiplier in terms of the shear strain rate as follows:

$$\left.\begin{array}{lll} \dot{\gamma}^{p\alpha} \neq 0 & \text{for} & \dot{\lambda}^{\alpha} > 0 \\ \dot{\gamma}^{p\alpha} = 0 & \text{for} & \dot{\lambda}^{\alpha} \leq 0 \end{array}\right\} \tag{19.122}$$

The deformation analysis by the forward-Euler calculation method is performed as follows:

(1) First calculate the plastic multipliers $\dot{\lambda}^{\alpha}$ by solving Eq. (19.117) for the input of the strain rate $\mathbf{d}$.
(2) If $\dot{\lambda}^{\alpha}$ is positive, calculate the plastic shear strain rate $\dot{\gamma}^{p\alpha} = n^{\alpha}\dot{\lambda}^{\alpha}$, the critical shear stress rate $\dot{\tau}_{y}^{\alpha}$ by Eq. (19.105) and the kinematic hardening rate $\dot{\chi}^{\alpha}$ by Eq. (19.109), the rate of normal-yield shear ratio $\dot{r}^{\alpha}$ by Eq. (19.110), the resolved shear stress rate $\dot{\tau}^{\alpha}$ by Eq. (19.32), the Jaumann rate of the Kirchhoff stress $\overset{\circ}{\boldsymbol{\tau}}{}^{w}$ by Eq. (19.54) and the rates of the base vectors $\dot{\mathbf{s}}^{\alpha}$, $\dot{\mathbf{n}}^{\alpha}$ of slip system by substituting Eq. (19.25) into Eq. (19.12). Then, update all these variables.
(3) If $\dot{\lambda}^{\alpha}$ is negative, set $\dot{\tau}_{y}^{\alpha} = 0$, $\dot{\chi}^{\alpha} = 0$, and calculate $\dot{\tau}^{\alpha}$ by Eq. (19.32), $\overset{\circ}{\boldsymbol{\tau}}{}^{w}$ by Eq. (19.54) and $\dot{\mathbf{s}}^{\alpha}$, $\dot{\mathbf{n}}^{\alpha}$ by substituting Eq. (19.25) into Eq. (19.12) under setting $\dot{\gamma}^{p\alpha} = 0$. Then, update all these variables. Thereafter, update r^{α} by Eq. (19.101).
(4) Move to the calculation for the next incremental step in which the updated values obtained in the above-mentioned processes are substituted.

19.9 Subloading-Overstress-Crystal Plasticity Model

Based on the extension of the overstress model by the subloading surface model in Eq. (13.29) or (13.30), let the viscoplastic slip rate $\overset{\bullet}{\gamma}^{vp\alpha}$ be given by

$$\overset{\bullet}{\gamma}^{vp\alpha} = \frac{1}{\mu_{cs}} \frac{\langle r^\alpha - r_s^\alpha \rangle^n}{r_{cm} - r^\alpha} n^\alpha \tag{19.123}$$

or

$$\overset{\bullet}{\gamma}^{vp\alpha} = \frac{1}{\mu_{cs}} \frac{\left\langle \exp[n(r^\alpha - r_s^\alpha)] - 1 \right\rangle}{r_{cm} - r^\alpha} n^\alpha \tag{19.124}$$

where μ_{cs} is the material constant standing for the *crystalline viscous coefficient*, $r_{cm}(\gg 1)$ is the material constant, called the *limit dynamic-loading ratio*, specifying the maximum value of r^α renamed as the *dynamic-loading ratio*, and $n(\gg 1)$ is the material constant.

The evolution rule of the *subloading ratio* $r_s^\alpha (0 \leq r_s^\alpha \leq 1)$ is given by

$$\left. \begin{array}{lll} \overset{\bullet}{r}_s{}^\alpha = U(r_s^\alpha)|\overset{\bullet}{\gamma}^{vp\alpha}| & \text{for} & r^\alpha > r_s^\alpha \, (\overset{\bullet}{\gamma}^{vp\alpha} \neq 0) \\ r_s^\alpha = r^\alpha = |\tau^\alpha - \chi^\alpha|/\tau_y^\alpha & \text{for} & \text{others} \, (\overset{\bullet}{\gamma}^{vp\alpha} = 0) \end{array} \right\} \tag{19.125}$$

following Eq. (19.110), where the function $U(r_s^\alpha)$ is given as

$$U(r_s^\alpha) = u_c \cot\left[(\pi/2) r_s^{\alpha n_c}\right] \tag{19.126}$$

The smooth resolved shear stress versus crystalline plastic shear strain curve is described always as shown in Fig. 19.6.

The evolution rule of the internal variables are given by replacing the plastic shear strain rate in the elastoplastic sliding equation to the viscoplastic shear strain rate. Then, the rate of critical shear stress is given from Eq. (19.105) as

$$\overset{\bullet}{\tau}_y{}^\alpha = \sum_{\beta=1}^{n} h_{\alpha\beta} |\overset{\bullet}{\gamma}^{vp\beta}| \tag{19.127}$$

$$h_{\alpha\beta} = q h(\gamma^{vp}) + (1-q) h(\gamma^{vp}) \delta_{\alpha\beta} = (h_{\beta\alpha}) \; (1 \leq q \leq 1.4) \tag{19.128}$$

$$h(\gamma^{vp}) = h_0 \mathrm{sech}^2\left(\frac{h_0 \gamma^{vp}}{\tau_s - \tau_{y0}}\right), \gamma^{vp} \equiv \sum_{\beta=1}^{n} \int_0^t |\overset{\bullet}{\gamma}^{vp\beta}| dt \tag{19.129}$$

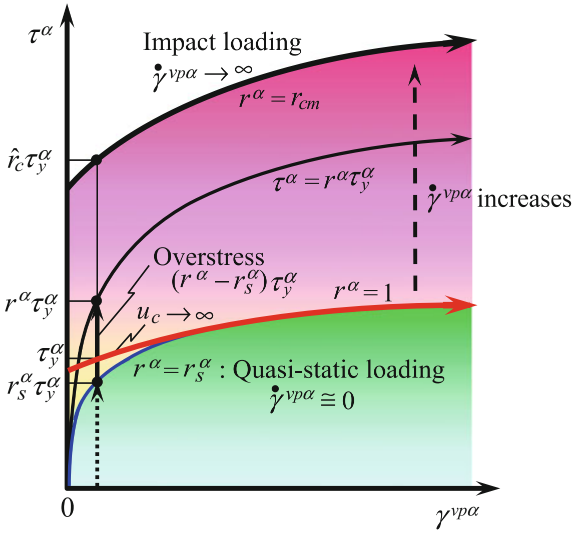

Fig. 19.6 Resolved shear stress versus crystalline plastic shear strain curve predicted by subloading-overstress-crystal plasticity model

and the rate of shear kinematic hardening variable is given from Eq. (19.109) as

$$\mathring{\chi}^\alpha = c_\chi\left(\mathring{\gamma}^{vp\alpha} - \frac{1}{\zeta_\chi\tau_y^\alpha}|\mathring{\gamma}^{vp\alpha}|\chi^\alpha\right) \tag{19.130}$$

$\mathring{\boldsymbol{\tau}}^w$ and $\mathring{\tau}^\alpha$ are given following Eqs. (19.54) and (19.32) by

$$\mathring{\boldsymbol{\tau}}^w = \mathbf{E} : \mathbf{d} - \sum_{\beta=1}^{n} \boldsymbol{\Xi}^\beta \mathring{\gamma}^{vp\beta} \tag{19.131}$$

$$\mathring{\tau}^\alpha = \boldsymbol{\Xi}^\alpha : \left(\mathbf{d} - \sum_{\beta=1}^{n} \mathbf{p}^\beta \mathring{\gamma}^{vp\beta}\right) \tag{19.132}$$

The elastic velocity gradient is given following Eq. (19.25) by

$$\boldsymbol{l}^* = \boldsymbol{l} - \boldsymbol{l}^{vp} = \boldsymbol{l} - \sum_{\beta=1}^{n} (\mathbf{p}^\beta + \mathbf{q}^\beta)\mathring{\gamma}^{vp\beta} \tag{19.133}$$

The deformation analysis by the forward-Euler calculation method is performed as follows:

(1) For $r^\alpha > r_s^\alpha$, calculate the crystalline slip rate $\dot{\gamma}^{vp\alpha}$ by Eq. (19.123) or (19.124), the rate of critical shear stress $\dot{\tau}_y^\alpha$ by Eq. (19.127), the rate of shear kinematic hardening variable $\dot{\chi}^\alpha$ by Eq. (19.130), the rate of resolved shear stress $\dot{\boldsymbol{\tau}}^\alpha$ by Eq. (19.132), the rate of subloading shear ratio $\dot{r}_s^\alpha$ by Eq. $(19.125)_1$, the Jaumann rate of the Kirchhoff stress $\overset{\circ}{\boldsymbol{\tau}}{}^w$ by Eq. (19.131) and the rates of the base vectors $\dot{\mathbf{s}}^\alpha$, $\dot{\mathbf{n}}^\alpha$ of slip system by substituting Eq. (19.133) into Eq. (19.12). Thereafter, calculate r^α by Eq. (19.101).

(2) For the other leading to $\dot{\gamma}^{vp\alpha} = 0$, set $\dot{\tau}_y^\alpha = 0$, $\dot{\chi}^\alpha = 0$, and calculate $\dot{\tau}^\alpha$ by Eq. (19.132), $\overset{\circ}{\boldsymbol{\tau}}{}^w$ by Eq. (19.131) and $\dot{\mathbf{s}}^\alpha$, $\dot{\mathbf{n}}^\alpha$ by substituting Eq. (19.133) into Eq. (19.12) under setting $\dot{\gamma}^{vp\alpha} = 0$. Then, update all these variables. Further, calculate r^α by Eq. (19.101) and set $r_s^\alpha = r^\alpha$.

(3) Move to the calculation for the next incremental step in which the updated values obtained in the above-mentioned processes are substituted.

19.10 Extension to Description of Cyclic Loading Behavior

The crystal plasticity model formulated in the preceding sections is based on the initial subloading surface model in which the similarity-center of the shear normal-yield and the shear subloading regions, i.e. the shear elastic-core is fixed at the shear kinematic hardening variable point. Therefore, unrealistically large shear strain accumulation is predicted, while open hysteresis loops are depicted as illustratively shown in Fig. 19.7. As described in Sect. 9.1. It will be extended to describe cyclic loading behavior by letting the similarity-center of the shear normal-yield and the shear subloading regions move with a plastic shear strain as shown in Fig. 19.7. The extended shear crystalline model formulated by Hashiguchi (2015) will be described in this section.

The subloading shear region is given instead of Eq. (19.101) as follows:

$$|\bar{\tau}^\alpha| = r^\alpha \tau_y^\alpha \tag{19.134}$$

where

$$\bar{\tau}^\alpha \equiv \tau^\alpha - \bar{\chi}^\alpha \tag{19.135}$$

$\bar{\chi}^\alpha$ stands for the conjugate (similar) point in the shear subloading shear region to the point χ^α in the normal-yield shear region. By letting c^α denote the similarity-center of the shear normal-yield and the shear subloading regions, which

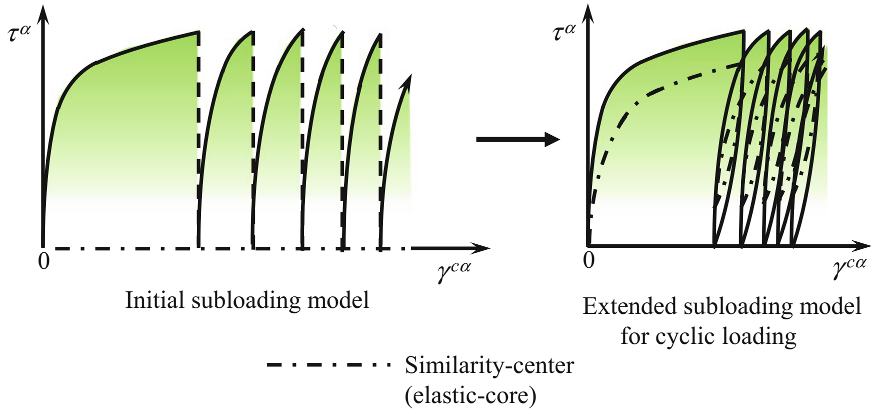

Fig. 19.7 Modification of subloading model to describe cyclic loading behavior

is called *shear elastic-core* since the most elastic shear behavior is induced when the resolved shear stress lies on it fulfilling $r^{\alpha} = 0$, the following relations hold by virtue of the similarity of the shear subloading region to the shear normal-yield region (see Fig. 19.8).

$$\left.\begin{array}{l} \bar{c}^{\alpha} \equiv c^{\alpha} - \bar{\chi}^{\alpha}, \hat{c}^{\alpha} \equiv c^{\alpha} - \chi^{\alpha} \\ \bar{c}^{\alpha} = r^{\alpha}\hat{c}^{\alpha} \end{array}\right\} \tag{19.136}$$

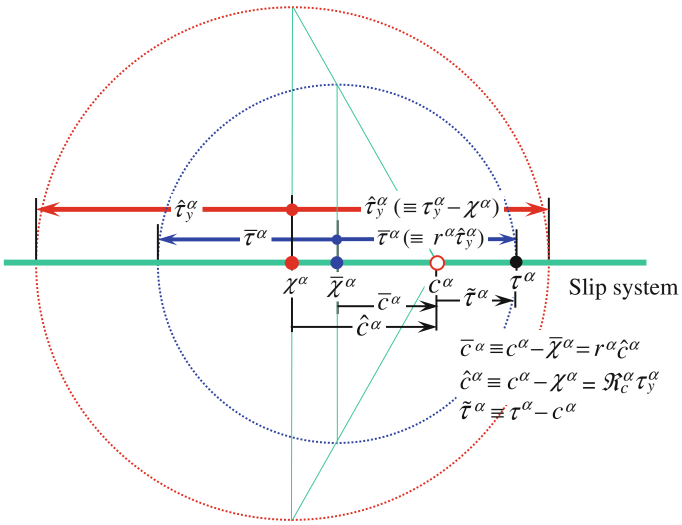

Fig. 19.8 Resolved and critical shear stresses, shear back-stress and shear elastic-core in slip system

It follows from Eqs. (19.135) and (19.136) that

$$\bar{\chi}^{\alpha} = c^{\alpha} - r^{\alpha}\hat{c}^{\alpha} \tag{19.137}$$

$$\bar{\tau}^{\alpha} = \tilde{\tau}^{\alpha} + r^{\alpha}\hat{c}^{\alpha} \tag{19.138}$$

where

$$\tilde{\tau}^{\alpha} \equiv \tau^{\alpha} - c^{\alpha} \tag{19.139}$$

The associated flow rule for the extended shear subloading region is adopted for the plastic shear strain rate as follows:

$$\overset{\bullet}{\gamma}{}^{p\alpha} = \overset{\bullet}{\lambda}{}^{\alpha}\bar{n}^{\alpha} \ (\overset{\bullet}{\lambda}{}^{\alpha} \geq 0) \ (|\overset{\bullet}{\gamma}{}^{p\alpha}| = \overset{\bullet}{\lambda}{}^{\alpha}) \tag{19.140}$$

where

$$\bar{n}^{\alpha} \equiv \frac{\partial|\bar{\tau}^{\alpha}|}{\partial\tau^{\alpha}} = \frac{\bar{\tau}^{\alpha}}{|\bar{\tau}^{\alpha}|} = \mathrm{sign}(\bar{\tau}^{\alpha}) \ (|\bar{n}^{\alpha}| = 1) \tag{19.141}$$

The shear kinematic hardening rule is given from Eq. (19.109) with Eq. (19.140) as

$$\overset{\bullet}{\chi}{}^{\alpha} = c_{\chi}\left(\overset{\bullet}{\gamma}{}^{p\alpha} - \frac{1}{\zeta_{\chi}\tau_y^{\alpha}}|\overset{\bullet}{\gamma}{}^{p\alpha}|\chi^{\alpha}\right) = c_{\chi}\overset{\bullet}{\lambda}{}^{\alpha}\left(\bar{n}^{\alpha} - \frac{1}{\zeta_{\chi}\tau_y^{\alpha}}\chi^{\alpha}\right) \tag{19.142}$$

Now, let the following shear *elastic-core region* be introduced, which always passes through the *shear elastic-core* c^{α} and maintains the similarity to the shear normal-yield surface with respect to the shear kinematic-hardening variable χ^{α}.

$$\hat{c}^{\alpha} = \Re_c^{\alpha}\tau_y^{\alpha}, \ \text{i.e.}\Re_c^{\alpha} = \hat{c}^{\alpha}/\tau_y^{\alpha} \tag{19.143}$$

where $\Re_c^{\alpha}$ designates the ratio of the size of the shear elastic-core region to the normal-yield region (see Fig. 19.8) so that let it be called the *shear elastic-core yield ratio*. Then, let it be postulated that the shear elastic-core can never reach the shear normal-yield region designating the fully-plastic shear state so that the shear elastic-core does not go over the following *limit shear elastic-core region.*

$$\hat{c}^{\alpha} = \xi_c\tau_y^{\alpha} \tag{19.144}$$

where $\xi_c \ (<1)$ is material parameter and the following inequality must be satisfied.

$$\hat{c}^{\alpha} \leq \xi_c\tau_y^{\alpha}, \ \text{i.e.}\Re_c^{\alpha} \leq \xi_c \tag{19.145}$$

The evolution rule of the shear elastic-core is given analogously to Eq. (19.15) as follows:

$$\overset{\bullet}{c}^{\alpha} = c_c\left(\overset{\bullet}{\gamma}^{p\alpha} - \frac{\mathfrak{R}_c^{\alpha}}{\xi_c}|\overset{\bullet}{\gamma}^{p\alpha}|\hat{n}_c^{\alpha}\right) = c_c\overset{\bullet}{\lambda}^{\alpha}\left(\bar{n}^{\alpha} - \frac{\mathfrak{R}_c^{\alpha}}{\xi_c}\hat{n}_c^{\alpha}\right) \tag{19.146}$$

where c_c is the material constant and

$$\hat{n}_c \equiv \frac{\hat{c}^{\alpha}}{|\hat{c}^{\alpha}|}\ (|\hat{n}_c| = 1) \tag{19.147}$$

The material-time derivative of Eq. (19.134) reads:

$$\bar{n}^{\alpha}(\overset{\bullet}{\tau}^{\alpha} - \overset{\bullet}{\bar{\chi}}^{\alpha}) = r^{\alpha}\overset{\bullet}{\tau}_y{}^{\alpha} + \overset{\bullet}{r}^{\alpha}\tau_y^{\alpha} \tag{19.148}$$

where $\overset{\bullet}{\bar{\chi}}^{\alpha}$ is described from Eq. (19.137) as

$$\overset{\bullet}{\bar{\chi}}^{\alpha} = r^{\alpha}\overset{\bullet}{\chi}^{\alpha} + (1 - r^{\alpha})\overset{\bullet}{c}^{\alpha} - \overset{\bullet}{r}^{\alpha}\hat{c}^{\alpha} \tag{19.149}$$

Substituting Eq. (19.149) into Eq. (19.148), one has

$$\bar{n}^{\alpha}\left\{\overset{\bullet}{\tau}^{\alpha} - \left[r^{\alpha}\overset{\bullet}{\chi}^{\alpha} + (1 - r^{\alpha})\overset{\bullet}{c}^{\alpha} - \overset{\bullet}{r}^{\alpha}\hat{c}^{\alpha}\right]\right\} = r^{\alpha}\overset{\bullet}{\tau}_y^{\alpha} + \overset{\bullet}{r}^{\alpha}\tau_y^{\alpha} \tag{19.150}$$

which is rewritten as

$$\bar{n}^{\alpha}\overset{\bullet}{\tau}^{\alpha} = \bar{n}^{\alpha}r^{\alpha}\overset{\bullet}{\chi}^{\alpha} + \bar{n}^{\alpha}(1 - r^{\alpha})\overset{\bullet}{c}^{\alpha} - \bar{n}^{\alpha}\overset{\bullet}{r}^{\alpha}\hat{c}^{\alpha} + r^{\alpha}\overset{\bullet}{\tau}_y^{\alpha} + \overset{\bullet}{r}^{\alpha}\tau_y^{\alpha} \tag{19.151}$$

i.e.

$$\overset{\bullet}{\tau}^{\alpha} = \bar{n}^{\alpha}r^{\alpha}\overset{\bullet}{\tau}_y^{\alpha} + r^{\alpha}\overset{\bullet}{\chi}^{\alpha} + (1 - r^{\alpha})\overset{\bullet}{c}^{\alpha} + (\bar{n}^{\alpha}\tau_y^{\alpha} - \hat{c}^{\alpha})\overset{\bullet}{r}^{\alpha} \tag{19.152}$$

Here, noting the relation

$$\begin{aligned}\bar{n}^{\alpha}\tau_y^{\alpha} - \hat{c}^{\alpha} &= \frac{\bar{\tau}^{\alpha}}{|\bar{\tau}^{\alpha}|}\frac{|\bar{\tau}^{\alpha}|}{r^{\alpha}} - \frac{\bar{c}^{\alpha}}{r^{\alpha}} = \frac{\bar{\tau}^{\alpha} - \bar{c}^{\alpha}}{r^{\alpha}} \\ &= \frac{(\tau^{\alpha} - \bar{\chi}^{\alpha}) - (c^{\alpha} - \bar{\chi}^{\alpha})}{r^{\alpha}} = \frac{\tilde{\tau}^{\alpha}}{r^{\alpha}}\end{aligned} \tag{19.153}$$

Equation (19.152) is rewritten as

$$\overset{\bullet}{\tau}^{\alpha} = \bar{n}^{\alpha}r^{\alpha}\overset{\bullet}{\tau}_y^{\alpha} + r^{\alpha}\overset{\bullet}{\chi}^{\alpha} + (1 - r^{\alpha})\overset{\bullet}{c}^{\alpha} + \frac{\overset{\bullet}{r}^{\alpha}}{r^{\alpha}}\tilde{\tau}^{\alpha} \tag{19.154}$$

Substituting Eqs. (19.105), (19.110), (19.142) and (19.146) into Eq. (19.154), it follows that

$$\begin{aligned}\overset{\bullet}{\tau}{}^{\alpha} = \bar{n}^{\alpha} r^{\alpha} \sum_{\beta=1}^{n} h_{\alpha\beta} \dot{\lambda}^{\beta} + r^{\alpha} c_{\chi} \dot{\lambda}^{\alpha} \left(\bar{n}^{\alpha} - \frac{1}{\zeta_c \tau_y^{\alpha}} \chi^{\alpha} \right) \\ + (1 - r^{\alpha}) c_c \dot{\lambda}^{\alpha} (\bar{n}^{\alpha} - \frac{\Re_c^{\alpha}}{\xi_c} \hat{n}_c^{\alpha}) + \frac{U(r^{\alpha})}{r^{\alpha}} \tilde{\tau}^{\alpha} \dot{\lambda}^{\alpha}\end{aligned} \tag{19.155}$$

which is rewritten as

$$\overset{\bullet}{\tau}{}^{\alpha} - \sum_{\beta=1}^{n} \bar{h}_{\alpha\beta} \dot{\lambda}^{\beta} = 0 \tag{19.156}$$

where

$$\begin{aligned}\bar{h}_{\alpha\beta} \equiv \bar{n}^{\alpha} r^{\alpha} h_{\alpha\beta} + r^{\alpha} c_{\chi} \left(\bar{n}^{\alpha} - \frac{1}{\zeta_{\chi} \tau_y^{\alpha}} \chi^{\alpha} \right) \delta_{\alpha\beta} \\ + (1 - r^{\alpha}) c_c \left(\bar{n}^{\alpha} - \frac{\Re_c^{\alpha}}{\xi_c} \hat{n}_c^{\alpha} \right) \delta_{\alpha\beta} + \frac{U(r^{\alpha})}{r^{\alpha}} \tilde{\tau}^{\alpha} \delta_{\alpha\beta}\end{aligned} \tag{19.157}$$

The overall constitutive equation itself described in Sect. 19.8 holds only with the replacement of $\bar{M}_{\alpha\beta}$ to the following equation.

$$\bar{M}_{\alpha\beta} \equiv \bar{h}_{\alpha\beta} + \boldsymbol{\Xi}^{\alpha} : \mathbf{p}^{\beta} \bar{n}^{\beta} (\neq \overline{M}_{\beta\alpha}) \tag{19.158}$$

References

Anand L, Kothari M (1996) A computational procedure for rate-independent crystal plasticity. J Mech Phys Solids 44:525–558

Asaro RJ (1983) Micromechanics of crystals and polycrystals. Adv Appl Mech 23

Asaro RJ, Needleman A (1985) Texture development and strain hardening in rate dependent polycrystals. Acta Metall 33:923–953

Asaro RJ, Rice JR (1977) Strain localization in ductile single crystals. J Mech Phys Solids 25:309–338

Bassani JL, Wu TY (1991) Latent hardening in single crystals II: theory analytical characterization and predictions. Proc Royal Soc London A 435:21–41

Darrieulat M, Piot D (1996) A method of generalized analytical yield surfaces of crystalline materials. Int J Plast 12:575–610

Franciosi P, Zaoui A (1991) Crystal hardening and the issue of uniqueness. Int J Plast 7:295–311

Gambin W (1991) Refined analysis of elastic-plastic crystals. Int J Solids Struct 29:2013–2021

Gambin W (2001) Plasticity and textures. Kluwer Academic Publishers, Dordrecht

Gambin W, Barlat F (1997) Modeling of deformation texture development based on rate independent crystal plasticity. Int J Plast 13:75–85

Golub GH, Van Loan CF (2013) In: Matrix computations, 4th edn. John Hopkins University Press. Baltimore, Maryland
Harder J (1999) A crystallographic model for the study of local deformation processes in polycrystals. Int J Plast 15:605–624
Hashiguchi K (2015) Crystal plasticity based on extended subloading surface model. In: Proceedings of 2nd science meeting of Kyushu Branch of Society of Material Science, Japan, B17
Havner KS (1982) The theory of finite plastic deformation of crystalline solids. In Mechanics of solids—Rodney Hill 60th anniversary volume, Pergamon, pp 265–302
Havner KS (1992) Finite plastic deformation of crystalline solids. Cambridge University Press, Cambridge
Hill R (1966) Generalized constitutive relations for incremental deformation of metal crystals. J Mech Phys Solids 14:95–102
Hill R, Rice JR (1972) Constitutive analysis of elastic-plastic crystals at arbitrary strain. J Mech Phys Solids 20:401–413
Hosford WF (1974) A generalized isotropic yield criterion. J Appl Mech (ASME) 41:607–609
Hosford WF (2009) Mechanical behavior of solids. Cambridge University Press, Cambridge
Hutchinson JW (1976) Bounds and self-consistent estimates for creep of polycrystalline materials. Proc Roy Soc London A 348:101–127
Knockaert R, Chastel Y, Massoni (2000) Rate-independent crystalline plasticity, application to FCC materials. Int J Plast 16:179–198
Mandel J (1973) Equations constitutives directeurs dans les milieux plastiques at viscoplastiques. Int J Solids Struct 9:725–740
Mandel J (1974) Director vectors and constitutive equations for plastic and viscoplastic media. In: Sawczuk A (ed) Problems of plasticity, proceedings of international symposium foundation of plasticity. Noordhoff Int. Publ., Leyden, Netherland, pp 135–141
Miehe C, Schroder J (2001) A comparative study of stress update algorithms for rate-independent and rate-dependent crystal plasticity. Int J Numer Meth Eng 50:273–298
Nakada Y, Keh AS (1966) Latent hardening in iron single crystals. Acta Metall 14:961–973
Peirce D, Asaro JR, Needleman A (1982) Overview 21: an analysis of nonuniform and localized deformation in ductile single crystals. Act Metall 30:1087–1119
Peirce D, Asaro JR, Needleman A (1983) Overview 32: material rate dependence and localized deformation in crystal solids. Act Metall 31:1951–1976
Press WH, Teukolsky SA, Vetterling WT, Flannery BP (1988) Numerical recipies. In: The art of scientific computing. Cambridge University Press, New York
Taylor GI (1938) Plastic strain in metals. J Inst Metals 62:307–324
Xu B, Jiang Y (2004) A cyclic plasticity model for single crystals. Int J Plast 20:2161–2178
Yoshida K, Kuroda M (2012) Comparison of bifurcation and imperfection analyses of localized necking in rate-independent polycrystalline sheets. Int J Solids Struct 49:2073–2084
Zamiri A, Pourbogharat F (2010) A novel yield function for single crystal based on combined constraints optimization. Int J Plast 26:731–746
Zamiri A, Pourbogharat F, Barlat F (2007) An effective computational algorithm for rate-independent crystal plasticity based on a single crystal yield surface with an application to tube hydroforming. Int J Plast 23:1126–1147